Study of an LHD-like magnetic equilibrium configuration

École Polytechnique Fédérale de Lausanne

Master in Physics - Special Project for exchange visiting student

Martim Negalho Lisboa Simões (331201)

December 25th 2020

Abstract

In this paper I show the results of my semester project on magnetic fields inside stellerators. Concretely, I focused on a model of the magnetic field in the Large Helical Device (LHD). After going over some of fundamental concepts and properties of magnetic fields inside stellerators, I learned how to use STELLOPT to numerically explore magnetic configurations. This code allowed me to, given a discrete set of current carrying coils in space, compute the magnetic field it generates and follow its fieldlines inside some delimiting region or wall. I was then faced with the main goal for this part of the project: analyse the magnetic field structure generated by the LHD modelling coils provided, and discover where most of the heat is expected to be deposited. I succeeded in creating useful Poincaré Plots that tell me where the magnetic field confines the Plasma and where it doesn't. The fieldlines in the confining region were further described by the calculation of their rotational transform with respect to the magnetic axis. To study the which fieldlines eventually divert the plasma particles out, I had to come up with a type of stellerator wall shape satisfying a set of geometrical constraints, namely, having rectangular cross section. I then computed where the various fieldlines strike 2 different walls of said shape. Identifying, based on their connection length, only the plasma diverting fieldlines I was, therefore, able to pin out where the most energetic charged particles are expected to strike the wall. Nevertheless, I conclude that the walls I experimented with are not suitable boundaries for a turbulence simulating code that I am hoping to explore, because hot plasma particles will tend to accumulate in the corners of each cross section and turbulence simulating codes don't behave well in those situations. I have yet to find a wall that is compatible with this.

I. Introduction

The achievement of confined and controlled nuclear fusion has been on the prying eyes of the Plasma Physics community for over half a century. This quest has brought a wide collection of machines or reactors to life. All reactors are built with the intent of keeping hot plasma inside them for as much time as possible. This not only allows fusion reactions to occur but also sustains them. Physicists have therefore come up with several ways to confine hot plasma in reactors, but the most successful has been through the use of magnetic fields - magnetic confinement. Since a plasma is nothing but an overall neutral soup of charged particles, we can use the laws of electrodynamics to describe how it moves in a magnetic field. The well known expression for the force experienced by a single charged particle in a magnetic field is:

$$\boldsymbol{F} = q\left(\boldsymbol{E} + \boldsymbol{v} \times \boldsymbol{B}\right) \tag{1}$$

This is the Lorentz force, and from this expression we can deduce that a uniform magnetic field only accelerates a particle in directions perpendicular to it in such a way that the particle gyrates around a magnetic field line with a radius inversely proportional to the magnitude of the field and a frequency directly proportional to it. Strong magnetic fields thus keep particles moving fast in tiny circles around the same the fieldline. In other words, motion in a uniform magnetic field is bound in the perpendicular direction but free in the direction parallel to the field. This analysis still holds true for non uniform magnetic fields at the time scale of the gyration period. However, on larger timescales the particles tend to drift between magnetic field lines due to effects of curvature or gradient in magnitude of the magnetic field (in the absence of other, namely electric, forces), especially when the radius of curvature of the field or the characteristic length scale of change of its magnitude are comparable to the radius of gyration. Notwithstanding this, the previous analysis is enough to show that the study of magnetic field configurations is of crucial importance in the construction of a magnetic confinement fusion reactor. Magnetic field lines can act as average trajectories for the individual charged particles in a plasma. The collective kinematic effect of a plasma (by means of electromagnetic collisional forces) on one of its constituent particles is to move it between different field lines, changing its trajectory. Therefore, a strong magnetic field can not only be used to keep the hot plasma inside the reactor vessel but also as a route to divert energetic charged particles out of the hot plasma bulk, so as to extract the heat produced by fusion reactions.

Out of all proposed designs for reactors the most promising is the tokamak. A tokamak is an axis-symmetrical toroidal like vessel, inside which lies an also axis-symmetrical strong magnetic field configuration. In spite of the great physics performance of current tokamak experiments, all tokamak operations rely on macroscopic movement of the plasma itself to produce part of the confining magnetic field. Although a natural transport mechanism responsible for toroidal current is present in tokamaks - bootstrap current, the need for external current sources can't be bypassed. This is not only energetically inefficient but also implies the tokamak doesn't run in steady state. Any deviation from steady state is unwanted because kinetic instabilities will start to develop and the plasma behaviour will be much harder to predict and control.

Although the physics of tokamaks is constantly changing, with new problems and solutions emerging by the day, some physicists have followed a completely different path: the search of an intrinsically steady state operating reactor, in which kinetic disruptions are difficult to excite. Their efforts have culminated with the stellerator, the physics of which we will be exploring in this project.

II. Elements of stellerator Physics

The stellerator exploits an inherently 3-D magnetic field configuration and is decently described by a helix bent into a torus (a toroidal helix). This design has no axis-symmetry, making it harder to understand. There are currently 3 major stellerator experiments running, the Wendelstein 7-X in Germany, the Helically Symmetric experiment or HSX in the United States and the Large Helical Device or LHD in Japan. The latter will be our major focus.
According to [5] the magnetic field configuration of a stellerator has 3 components: a large axisymmetric toroidal field, $\boldsymbol{B_\varphi}(r,\theta)$, a moderate helical field with N_{FP} field symmetry, and a smaller axisymmetric vertical field $\boldsymbol{B_V}(r,\theta)$. By N_{FP} field symmetry we mean that the magnetic field is $\frac{2\pi}{N_{FP}}$ periodic in the toroidal angle φ, as N_{FP} is the number of field periods.
These configurations have great advantages when it comes to single particle confinement and stability, which will be explored later in the project. We are now ready to learn how to dissect a magnetic field inside a stellerator.

1. Magnetic Geometry inside a Stellerator

1.1 Magnetic Fieldlines

Magnetism is the effect of moving electric charge and/or spin magnetic moments. In classical electromagnetic theory, these effects are mediated through a magnetic field, whose source is a distribution of animated electric charged (current) or spin magnetic moments. In this project we will only deal with steady state current sourced magnetic fields and the fundamental equation to calculate a static magnetic field from a current distribution is the Biot-Savart law:

$$\boldsymbol{B}(\boldsymbol{r}) = \frac{\mu_0}{4\pi}\iiint_V d^3r' \frac{\boldsymbol{J}(\boldsymbol{r'}) \times (\boldsymbol{r}-\boldsymbol{r'})}{|\boldsymbol{r}-\boldsymbol{r'}|^3} \tag{2}$$

This equation is the magnetostatic solution to Maxwell's equations, of which one is particularly important when studying the magnetic geometry in a stellerator : Gauss's Law:

$$\boldsymbol{\nabla}\cdot\boldsymbol{B} = \boldsymbol{0} \tag{3}$$

A divergenceless vector field like $\boldsymbol{B}$ has no point sources. The lines (1-manifolds) whose derivative is the directing vector of the field - the vector field's fieldlines have, as a consequence, an important property: they are always closed, meaning they neither begin nor end. This allows us to classify a divergenceless vector field's fieldlines into one of two types, bounded and unbounded. Following a bounded fieldline in either direction will eventually get us to the same place where we started from, whereas following an unbounded fieldline will get us infinitely far away from the starting point. Unbounded fieldlines close at infinity.
Mathematically, a magnetic fieldline $\boldsymbol{\gamma}$ passing through point $\boldsymbol{r_0}$, can be parameterized by some real parameter s, and is defined by the following equations:

$$\begin{cases} \boldsymbol{\gamma}(s=0) = \boldsymbol{r_0} \\ \frac{d\boldsymbol{\gamma}}{ds} = \frac{\boldsymbol{B}}{|\boldsymbol{B}|} \end{cases} \tag{4}$$

In cylindrical coordinates this set of differential coordinates reads:

$$\begin{cases} \frac{dR}{ds} = \frac{B_R}{|\boldsymbol{B}|} \\ \frac{Rd\phi}{ds} = \frac{B_\phi}{|\boldsymbol{B}|} \\ \frac{dz}{ds} = \frac{B_z}{|\boldsymbol{B}|} \end{cases} \tag{5}$$

If we take $s=\phi$, the differential equations that need to be solved in order to find the fieldlines are:

$$\begin{cases} \frac{dR}{d\phi} = R\frac{B_R}{B_\phi} \\ \frac{dz}{d\phi} = R\frac{B_z}{B_\phi} \end{cases} \tag{6}$$

These equation are, of course, subject to some initial condition R_0, z_0 at $\phi=\phi_0$ that defines the point $\boldsymbol{r_0}$. One very useful property of these equations is that they are length scale invariant, meaning that if we send $R \to \lambda R$ and $z \to \lambda z$ given some scalar λ, the equations don't change, and the fieldlines' shape scales accordingly. This will be exploited to optimize simulations.

1.2 Flux Surfaces and Poincaré Plots

As a given bounded fieldline winds around the toroidal vessel which contains the stellerator it may either take a few turns to close or never close. In the latter case, the fieldline fills out either a surface , called a flux surface, or even a volume. A surface with normal $\hat{\boldsymbol{n}}$ such that $\boldsymbol{B}\cdot\hat{\boldsymbol{n}} = 0$ is called a flux surface.
As I have argued before, charged particles gyrate around magnetic fieldlines and move freely (in first approximation) parallel to them. A collection of charged particles following the same bounded fieldline will therefore tend to thermalize. Therefore, flux surfaces are good indicators of surfaces of constant temperature/pressure.

Inside a stellerator, flux surfaces are usually concentric around a single bounded fieldline that closes after one toroidal turn - the magnetic axis. This line doesn't need to be circular, and when this happens we say that the configuration has torsion.
A good way to represent this is through a Poincaré plot. This is a 2D plot mapping a given surface $\mathcal{S}$ (usually of constant toroidal angle in our case). Given a magnetic field $\boldsymbol{B}$, we follow a set of $\boldsymbol{B}$ fieldlines and record every intersection with the surface $\mathcal{S}$ as a point in the 2D plane representing it. Concentric fieldlines will trace out a set of concentric closed curves.
In the following example intersections of the same fieldline with the surface are points of the same color.

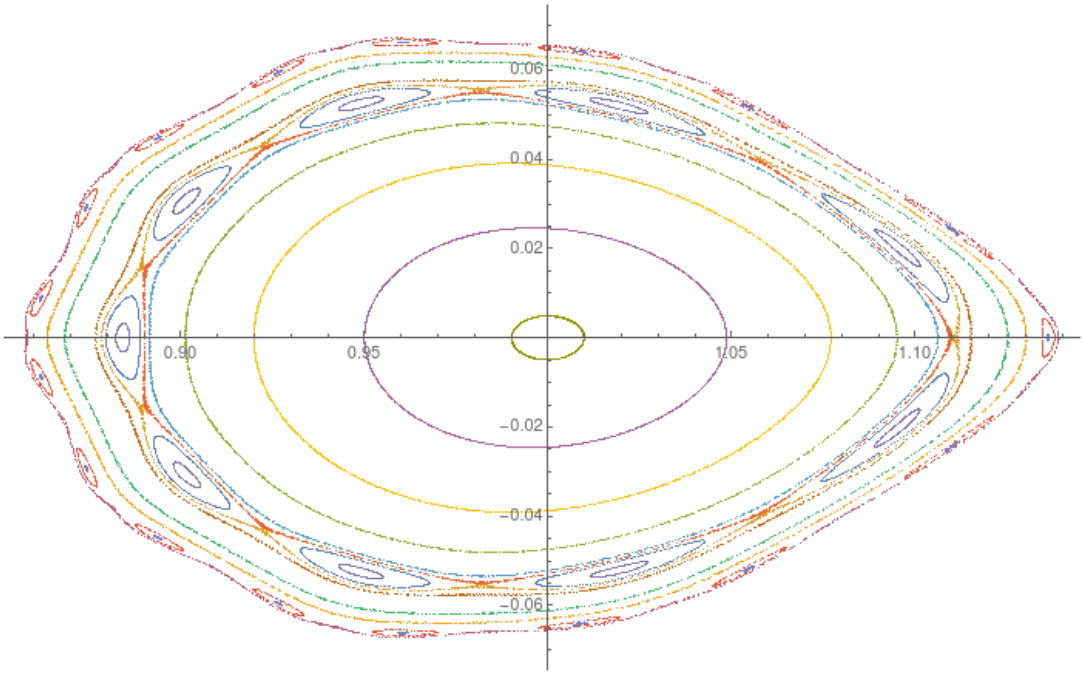

Figure 1: *Example of Poincaré Plot*

It is also possible that closed fieldlines concentric around a secondary magnetic axis form in between two flux surfaces that are concentric around the primary magnetic axis. When this happens we say that the fieldlines form magnetic island structures. This can be seen in the last figure.
Inside a stellerator the Poincaré Plot of the Magnetic field intersecting a plane of constant toroidal angle has 3 main regions of fieldlines, depending on how close to the magnetic axis they intersect the surface. The first region is characterized by closed curves, corresponding to bounded fieldlines that fill out flux surfaces. Fieldlines very close to the magnetic axis trace out ellipse like concentric curves. These closed curves deviate from an elliptic shape as we get away from the magnetic axis. Magnetic island structures then start to emerge in between flux surfaces. After this we get to the second region, where some fieldlines are bounded and trace flux surfaces, others are also bounded but fill out flux volumes, and others are unbounded, winding, nevertheless, many times around the torus before going going to infinity. This is the most important region since it contains those fieldlines that particles exiting the reactor will follow. Most of the work I will show revolves around understanding the geometry of these fieldlines inside a particular vessel. The final region is filled with unbounded field lines that exit the stellerator shortly after entering it, and appears in the Poincaré Plot as a disperse cloud of points. These fieldlines are not as important since the plasma, initially in the first region will slowly drift to the second region and exit the reactor through one of the fieldlines there, never reaching the last region.

1.3 Rotational Transform

Now that we are aware of the importance of flux surfaces, we define a quantity that helps us describe a given fieldline. Knowing that, to confine plasma, fieldlines need, not only, to wind around the torus, but also poloidally around the magnetic axis, let us introduce the Rotational Transform of a fieldline. This quantifies how many times a given, bounded, fieldline twists, on average, around the magnetic axis in every revolution around the torus. Let $(\Delta\theta)_k$ be the change in poloidal angle of a given fieldline around the magnetic axis in the k^{th} turn around the torus. Then the Rotational transform is, by definition:

$$\iota = \lim_{n\to\infty} \frac{\sum_{k=0}^{n} (\Delta\theta)_k}{2\pi n} \tag{7}$$

Note that a fieldline with $\iota = m/n$ a rational number closes after completing m poloidal turns around the magnetic axis over the course of n toroidal turns. These fieldlines, unlike those for which ι is irrational, don't fill a surface alone. A secondary magnetic axis is an excellent example of a fieldline of rational ι.

2. Walls, Strikepoints and Connection Length

Like any other reactor, the stellerator is built with the intent of extracting heat from fusion reactions that occur within it. As this energy is carried out of the stellerator by charged particles travelling along magnetic fieldlines, the magnetic geometry plays a central role in the design of the primary wall of the stellerator.
A magnetic fieldline inside a the wall of a stellerator is either completely bounded inside the wall or intersects the wall in two points. These intersections are called the fieldline's strikepoints.
We call the length of the fieldline inside the wall its connection length. Fieldlines with zero strikepoints have a infinite connection length (even if they close after a finite number of turns).
Since the magnetic field is everywhere in space, one might wonder which fieldlines actually carry the hot charged particles out of the vessel. These fieldline's striking points are the ones we are interested in, as they represent where heat will accumulate in the primary wall. Now, to know through which fieldlines will the hot plasma exit the reactor we need to go back to section 1.2. As the hot plasma is initially close to the magnetic axis, in the region where all fieldlines are bounded inside the wall and slowly drifts outward, the first fieldlines it encounters that will inevitably leave the vessel can be found in the second region. Thus, these are the fieldlines whose strikepoints describe heat accumulation.
In addition to knowing where in the wall these fieldlines hit, the angle at which they strike is also important - striking angle. The closer to 90° this angle is, the more energy is deposited at that strikepoint.

III. Modelling a Stellerator

To explore what kind of magnetic geometry is produced by a given current distribution, we need a way to calculate the magnetic field from said distribution using equation (2). Once we know the magnetic field everywhere we need also to follow its fieldlines, obtained from $\boldsymbol{B}$ through equations (6) and the initial condition. In addition to all of this, we also have to know where the magnetic fieldlines will deposit hot charged particles in a given wall. This wall has, therefore, to be modeled in such a way that allows for reconstruction of the strikepoints and the striking angle of various fieldlines incident on it.
The computational tool I used to numerically solve for the magnetic geometry produced by a current distribution is called STELLOPT.

1. STELLOPT Overview

STELLOPT is a "State-of-the-art stellerator optimization code" currently hosted on the Princeton University GitHub repository. It is built to simulate and optimize MHD equilibria to a set of target parameters, inherent to the stellerator design. It is a set of programs that can be compiled and executed separately or together. Each of them requires its own set of input files, and produces another set of output files. Among the many functionalities of STELLOPT, all of which are thoroughly documented in [1] and [2], I used STELLOPT for two things:

1. Calculate a Magnetic field from a current distribution.
2. Follow the fieldlines and analyse the magnetic geometry.

To aid in visualization, STELLOPT has a matlab library devoted to plotting the output of its codes.

1.1 Calculating a Magnetic Field - MAKEGRID

The MAKEGRID code, documented in [3], numerically solves equation (2), the Biot-Savart law of magnetostatics. This allows for prediction of the influence of the external loops of current in the plasma. As expected, its input has to be a description of the external current density. This is done through a "coils." file, in which a loop of current is encoded as a list of arrays of 4 numbers, each corresponding to a XYZ point in space, and a value for current at that point. Consecutive arrays in the list define the direction of the flow of current. Several coil groups can be defined in this file. They should be separated by a a line consisting of 4 zeros, a number indexing the group and the coil group name. All this is very well explained in [3].
In addition to the "coils." file, MAKEGRID needs to know where in space to calculate the magnetic field. This is done by specifying the maximum and minimum vertical and radial extent, as well as a number of toroidal cutplanes, in a cylindrical grid.
The primary output of MAKEGRID is a "mgrid" file, that contains the magnetic field produced by each of the coil groups individually, in each input cylindrical grid point. It is based on this file that fieldlines will be followed and the magnetic geometry is explored.

1.2 Following fieldlines in space - FIELDLINES

The FIELDLINES code, documented in [4], follows magnetic fieldlines inside a given domain, by solving equations (6).
As input, this code needs a description of the magnetic field inside a given domain, as well as the initial conditions (points in space) for the various fieldlines to be followed.
The magnetic field is best provided to the code through an mgrid file, the output of MAKEGRID. This file also comes with a toroidal domain which, by default, limits where in space fieldlines can be followed to. Notwithstanding this, there are other ways to specify the boundaries of the region where fieldlines can be followed, namely by encoding a wall through a "vessel" or "wall" file. I will

explain how to do this in the next section, as this is not documented in the STELLOPT website. Finally, the initial conditions for the fieldlines are supplied through an input namelist, which contains many things, namely the number of field periods, Initial conditions consist of a list of R,Z points, to which corresponds a interval in toroidal angle $[\varphi_{min}, \varphi_{max}]$.

Numerically, this code tries to follow the fieldlines between φ_{min} and φ_{max} but stops once they touch either the wall, or the limits of the supplied toroidal grid. It also gives the option of following the fieldlines backwards, by flipping the sign of φ_{max} (φ_{min} is usually taken to be around zero). The connection length of each fieldline between the starting and ending points is automatically calculated too. Another useful option this code has is to only record the striking points of the fieldlines, instead of their entirety. T

This code outputs a hdf5 file containing information about fieldlines starting in all the initial conditions. The hdf5 format is convenient to deal with large amounts of data. From it we can reconstruct the fieldlines inside the vessel, allowing for calculation of their striking points and the rotational transform.

2. Modelling a wall

A wall is a closed surface, that in this case fits inside a toroidal vessel. To model a surface in 3D we need to discretize it by providing a set of XYZ points belonging to it - its vertices. However, this is not enough. Just like when modelling a line a discrete set of points won't do unless you specify them in a given order or direction, the case of a closed surface is similar. You need a way to encode where the normal direction to the surface points to in space, at every point. This is done by supplying a list of triplets of vertices. Each triplet of vertices defines a plane tangent to the surface in that region. Essentially we are encoding a surface in 3D by a set of triangles patched together - its faces.

As an example I will show how to encode a quadrangular pyramid's surface. The base of this pyramid is a square of side 1 centered at the origin and lying in the xy plane, and the tip is at z = 1. There are many ways to choose the encoding vertices but, in the case of a pyramid, as all sides are flat, our best option is to go for the actual 5 vertices.

X	Y	Z
0.5	0.5	0
-0.5	0.5	0
-0.5	-0.5	0
0.5	-0.5	0
0	0	1

We then assume that the vertices are numbered by their order (the base vertices are 1,2,3,4 and the tip is 5) and proceed to discretizing the surface into triangular faces. A line with 1 2 3 represents a triangular face with vertices 1, 2 and 3. Since the base is a square it has to be subdivided into triangles. There are many ways to do so but 2 triangles are enough.

For the base face of the pyramid we get the following triangular patches: 1 2 3 and 1 3 4.

The remaining faces are triangles already, so there is not much left to do but write them as triplets of vertices. This is all the information needed to encode a surface in 3D, and from it we can calculate the normal direction to each patch using elementary linear algebra, since 3 points in space define a 2-plane.

Finally, to feed this information to STELLOPT we need to write a "vessel" file, which contains a name, a date and a line telling how many vertices and how many faces. For our pyramid example it would look something like this:

Quadrangular Pyramid Surface
Sun Feb 29 15:46:32 2023
5 6 # $\rightarrow$ number of vertices and faces

0.5	0.5	0
-0.5	0.5	0
-0.5	-0.5	0
0.5	-0.5	0
0	0	1
1	2	3
1	3	4
1	2	5
2	3	5
3	4	5
4	1	5

When we ask MATLAB to plot this we get our expected pyramid:

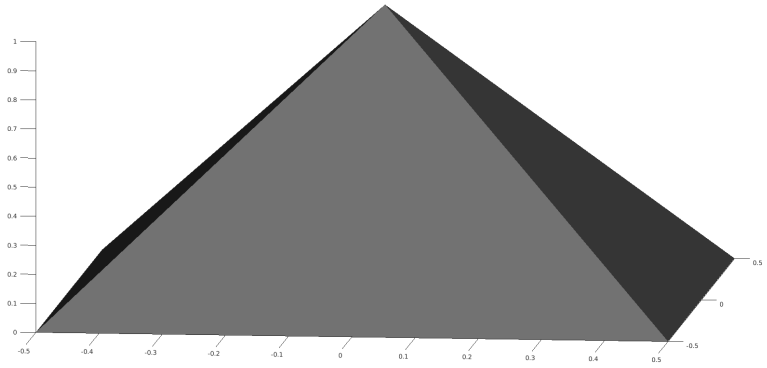

Figure 2: *Pyramid encoded in our wall file*

Speaking of plotting things in MATLAB, let's now learn how to visualize the outputs and inputs of STELLOPT.

3. Visualizing STELLOPT

As I have already stated, to aid in visualization of the output of STELLOPT, there exists a MATLAB library. Detailed information about each method can be found in its defining file. I used the following methods:

1. read_coils("coils."file name) → converts a the information in a "coils." file to a MATLAB data structure.
2. plot_coils(coils_data) → Plots the different coil groups encoded in the coil_data MATLAB structure as sets of closed loops in 3D space.
3. read_wall("vessel" filename) → stores the information of a "vessel" file in a matlab data structure
4. plot_wall(wall_data, option) → 3D plots the wall surface encoded in the wall_data MATLAB structure. The option argument allows for different ways of plotting the surface.
5. read_fieldlines("fieldlines.h5" hdf5 filename, optional "iota") → stores all the information about the magnetic field and its fieldlines encoded in a hdf5 file in a MATLAB data structure. The optional argument "iota" allows for calculation and storing of the rotational transform of each fieldlines with respect to the first fieldline (taken to be the magnetic axis).
6. plot_fieldlines(field_data, option) → probably the most important method in this list as it allows for visualization of fieldlines in many ways. The default option is to produce a Poincaré plot in the first cutplane given in the input (usually $\varphi = 0$). Other important options include "cutplane" and "phi", which are both used to specify in which fixed φ plane we want to produce a Poincaré plot. "skip" plots 1 in every N fieldlines, wher N is also given as input. "wall_strike" plots the wall in 3D, if one was fed as input of FIELDLINES, and shows not in which faces the fieldlines striked but also where they striked more directly (striking angle close to 90°). "strike_2D" shows the striking points as a function of toroidal and poloidal angles φ, θ.
7. plot_fieldlines_conn_length(folder name, option) → plots the various initial conditions of the followed fieldlines and gives each of them a color based on how long they stayed inside the vessel. It therefore needs as argument, a name of a folder containing the input file of FIELDLINES used (stored the initial conditions), as well as 2 hdf5 files storing the fieldlines followed forward and backward in φ, named "fieldlines_name.h5" and "fieldlines_name_rev.h5" respectively.

As most of the plotting methods were tailored to the geometry of the Wendelstein 7-X geometry (especially the "wall_strike" and "strike_2D" options of plot_fieldlines and the plot_fieldlines_conn_length) , I had to carefully read through them and make the necessary adjustments before using. Notwithstanding this, I still needed to create another method that, inspired in plot_fieldlines_conn_length, would plot the both strike points of every fieldline that touched the wall.

8. plot_strikepoints(folder name, option) → Plots the strikepoints of fieldlines followed both forward and backward. The option argument in this method will be explained later.

IV. Magnetic Geometry of the LHD

1. Sources of the Magnetic Field

The Large Helical Device (LHD) is a stellerator experiment located in Toki, Japan. The magnetic field has $N_{FP} = 10$, meaning $B(r, \varphi, z) = B(r, \varphi + \frac{2\pi}{10}, z)$. To achieve a magnetic field like this, the LHD has 2 loops of current in a toroidal helix shape (a helical line that lies on the surface of a torus) each with angular repetition period of $\frac{2\pi}{5}$. In order to have a magnetic field that is invariant under discrete rotations of multiples of $\frac{2\pi}{10}$, its source has to also be invariant under such rotations. Therefore, it is mandatory that these to toroidal helices be completely out of phase.
My starting point for this project is a "coils." file attempting to model this field. This file is inspired in [6], and has the toroidal helices with the desired symmetry properties. I started by plotting these current loops:

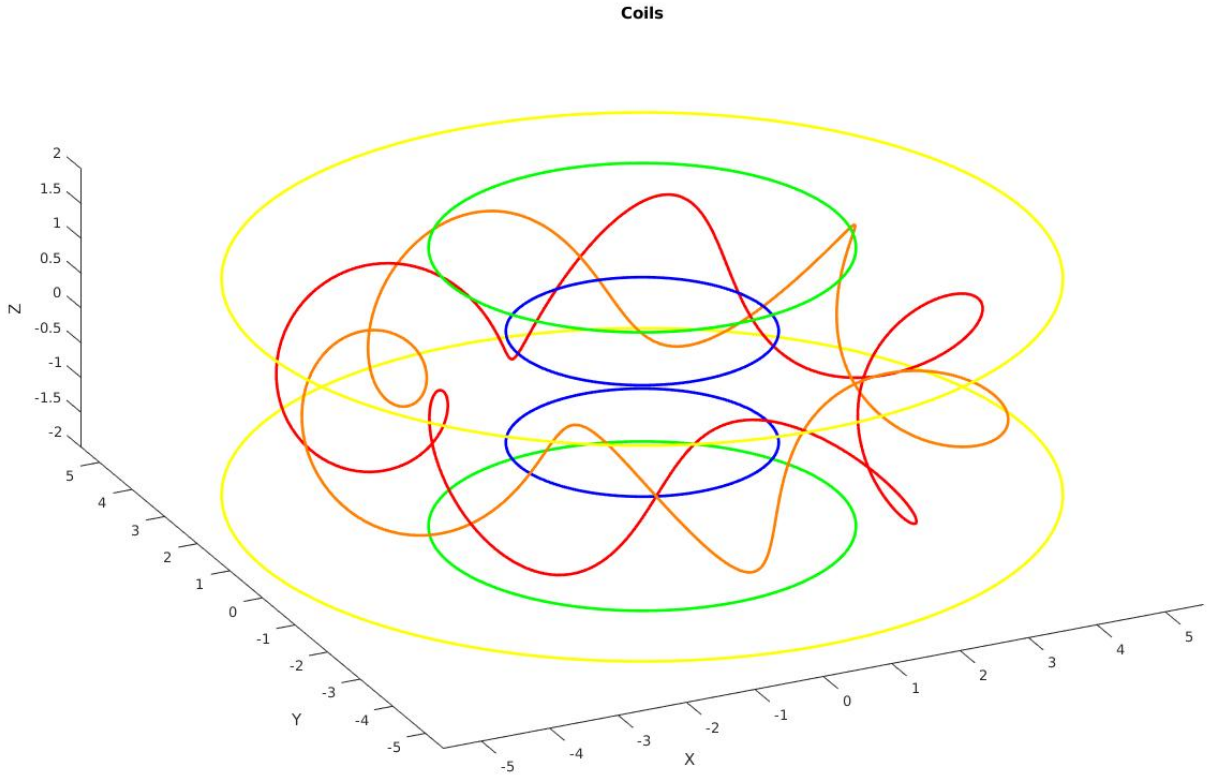

Figure 3: *Current loops modelling sources of the LHD magnetic field*

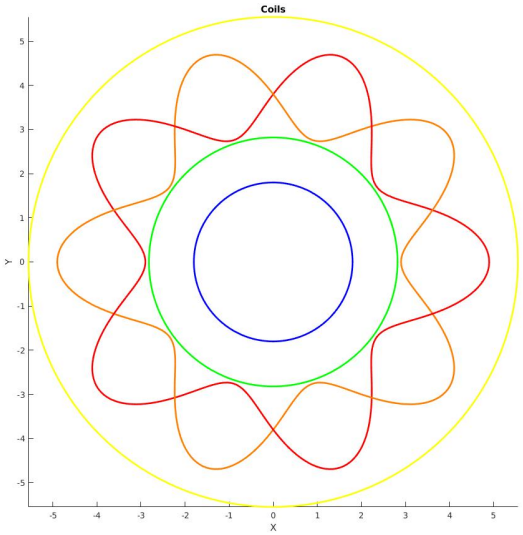

(1) *Top view*

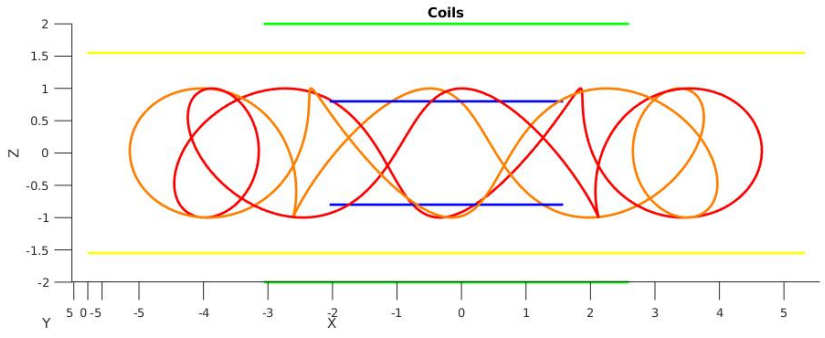

(2) *Side view*

In addition to the toroidal helices shown in Red and orange, the file also shows three pairs of circular loops symmetric to the xy plane Knowing that the helices this file were modeled like in [7], I set out o find the parametric equations of each coil. The circular coils are trivially modeled by:

$$\begin{cases} R(\varphi) = R_{C_i} \\ Z(\varphi) = Z_{C_i} \end{cases} \quad , \quad \varphi \in [0, 2\pi] \tag{8}$$

While for the toroidal helices the equations are:

$$\begin{cases} R(\varphi) = R_H \left(\varepsilon_R \cos\left(N\varphi + \alpha_R sin(N\varphi)\right) + 1\right) \\ Z(\varphi) = R_H \left(\varepsilon_Z \sin\left(N\varphi + \alpha_Z sin(N\varphi)\right)\right) \end{cases} \quad , \quad \varphi \in [0, 2\pi] \tag{9}$$

Where R_H is the radius of the center of the coils - major radius, $N = 5$ to assure the symmetry properties previously discussed, ε is how much how much a fraction of the major radius the minor radius is. Finally, parameter α is called pitch modulation (see [7]). To find these parameters I fitted the data in the coils file to these equations, using the method of least squares (implemented in the software ROOT). It is worth adding that to fit the data to the parametric equation of the toroidal helices I had first to divide Z by R , eliminating R_H. I then fitted Z/R to :

$$Q(\varphi) = \frac{\left(\varepsilon_Z \sin\left(N\varphi + \alpha_Z sin(N\varphi)\right)\right)}{\left(\varepsilon_R \cos\left(N\varphi + \alpha_R sin(N\varphi)\right) + 1\right)} \tag{10}$$

And used the result of this fit to find $\varepsilon_{R,Z}$ and $\alpha_{R,Z}$. To find R_H, I plugged these last values into equations (9) as initial estimates and fitted Z and R separately, always checking if the output fits were compatible to that o Q.
For the helical coils I got:

Coil	R_H	ε_R	ε_Z	α_R	α_Z	I
1 (red)	3.9	$0.2564 = \frac{1}{3.9}$	-0.2564	0.1	0.1	-5.4×10^6
2 (orange)	3.9	-0.2564	0.2564	-0.1	-0.1	-5.4×10^6

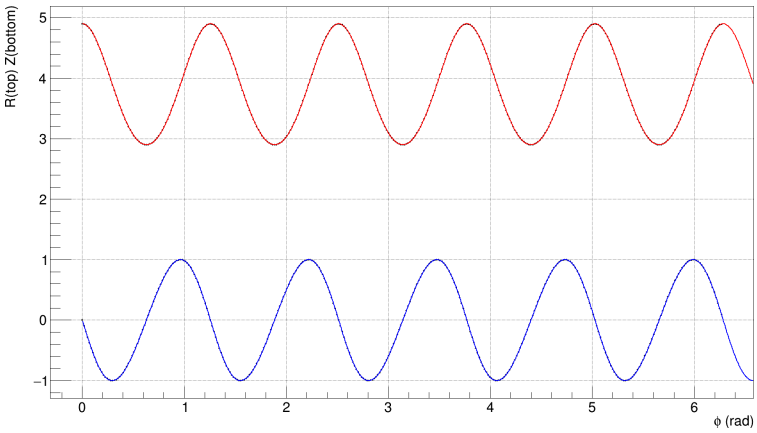

(1) *Red Coil*

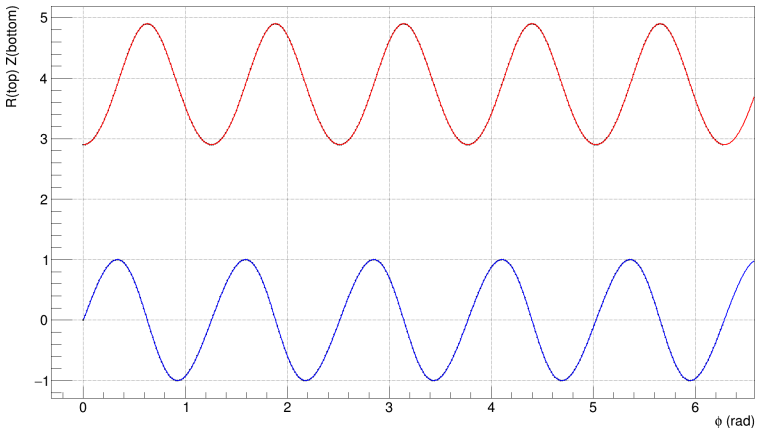

(2) *Orange coil*

Figure 5: *Fitting curve for R (top) and Z (bottom) for both helical coils*

The coils have a major radius of 3.9 and a minor radius of 1. The pitch modulation is 0.1 and all the relative signs are there to take the necessary phase shift in φ between the two coils into account. The final parameter I is the current in the loop. I will call the current in these helical coils I_0 and show the remaining currents as multiples of this. All the relative fitting errors were very small, meaning the fit was successful.
For the circular coils the relevant parameters are:

Coils	R_{C_i}	Z_{C_i}	I/I_0
3 (Yellow)	5.55	± 1.55	$-0.523(037)$
4 (Green)	2.82	± 2	$-0.126(3)$
5 (Blue)	1.8	± 0.8	0.5(4)

2. The Magnetic Field

Now that we have a clear idea of the current distribution giving rise to the magnetic field its time to feed it to STELLOPT's MAKEGRID and then start following some fieldlines with FIELDLINES. I used a grid spanning $R \in [1, 6]$ and $Z \in [-2.5, 2.5]$. These intervals were divided into 500 pieces each. As for the angle φ I discretized it in 360 degrees.

To produce a good Poincaré Plot you need to decide which fieldlines to follow. The process of deciding which initial conditions are good to explore the magnetic geometry is one of trial and error. On one hand you need to follow enough fieldlines to differentiate between different regimes. On the other, you can't afford (computationally) to follow as many fieldlines as you like in finite time, and a Poincaré Plot with too many fieldlines can become messy and lose information.

I opted to follow fieldlines that start in the $\varphi = 0$ plane and have $Z_{init} = 0$. This is a very conventional choice to produce clear and informative Poincaré Plots. The initial radius R_{init} is, therefore, a good parameter to label fieldlines, and differentiate between different types of them.

Without no further delay I will show you the Poincaré Plots I got using these kinds of initial conditions.

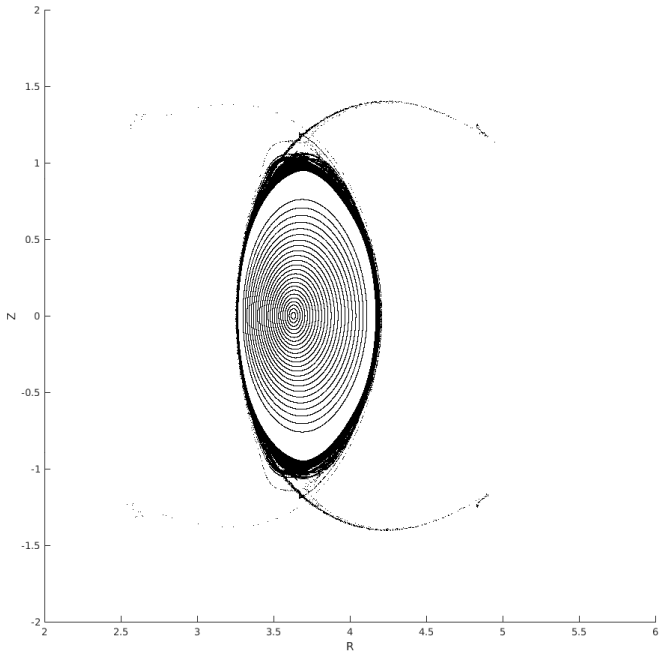

(1) $\varphi = 0°$

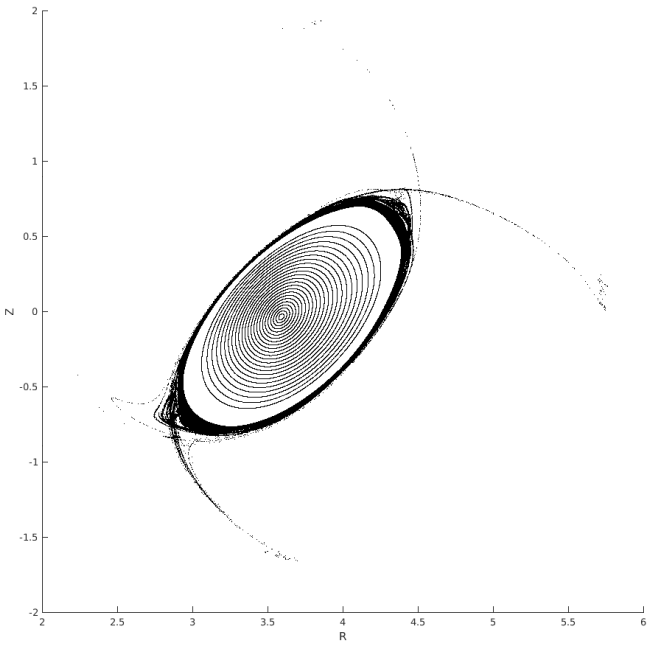

(2) $\varphi = 9°$

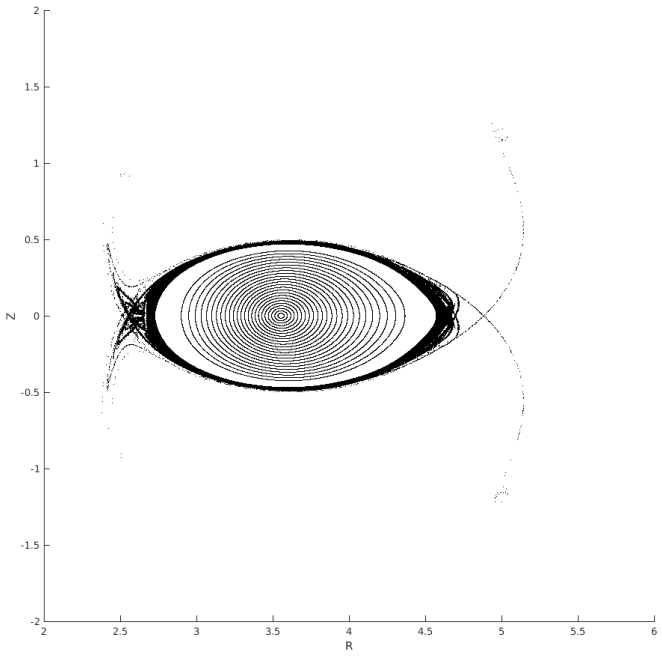

(3) $\varphi = 18°$

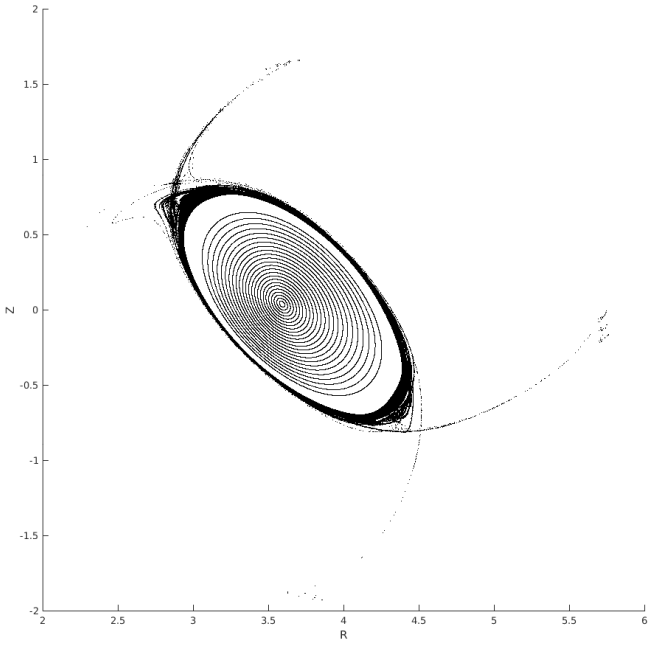

(4) $\varphi = 27°$

Figure 6: *Poincaré Plots for different cutplanes*

The first thing to note here is that there are clearly 2 regions of fieldlines. The regularity of concentric ellipse like closed curves clearly contrasts with the complex structure of nested magnetic islands embedded in stochasticity that can be observed in the outer rim and shown in detail in the next figure. It is worth noting that to explore the complexity of this last region I had to follow a much higher number of fieldlines starting in a very small interval in R_{init}. That is why the outer region looks, at a larger scale, like a black blur.

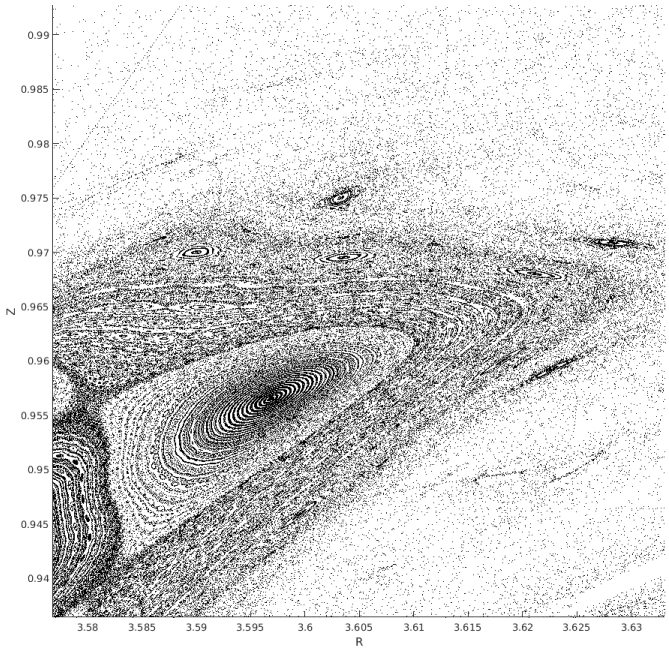

Figure 7: *Detail of the Poincaré Plot in the outer region for* $\varphi = 0$

The magnetic fieldline structure rotates poloidally 180° every field period of $\Delta\varphi = 36°$, morphing back into itself. This is the manifestation of the stellerator's field symmetry. This rotation is clockwise as expected, since the generating helical loops of current have $\varepsilon_R/\varepsilon_Z = -1$, meaning they also rotate clockwise.
We can also see that this configuration shows two pairs of diametrically opposed "leg" like structures, that rotate and morph with the rest. This is called a rotating double null and it is a fundamental characteristic of LHD like magnetic configurations. A plasma particle, initially confined in the central region of regular flux surfaces slowly drifts outward, reaching the stochastic region. When this happens the particle will eventually follow one fieldline that leads it to exit the vessel through one of these "legs". The point (or region around it) of intersection between these legs is called the X point, and in a real experiment we expect hot plasma to accumulate around the X point, leading to complex turbulent behaviour. The following figures show details of both X points in the $\varphi = 18°$ plane.

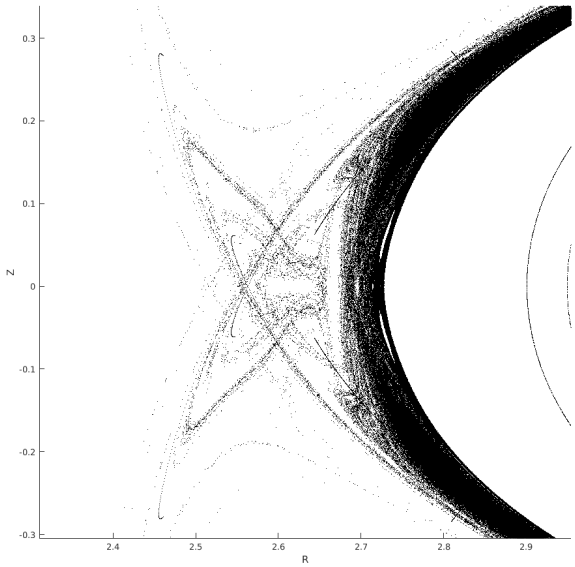

(1) *Left X point*

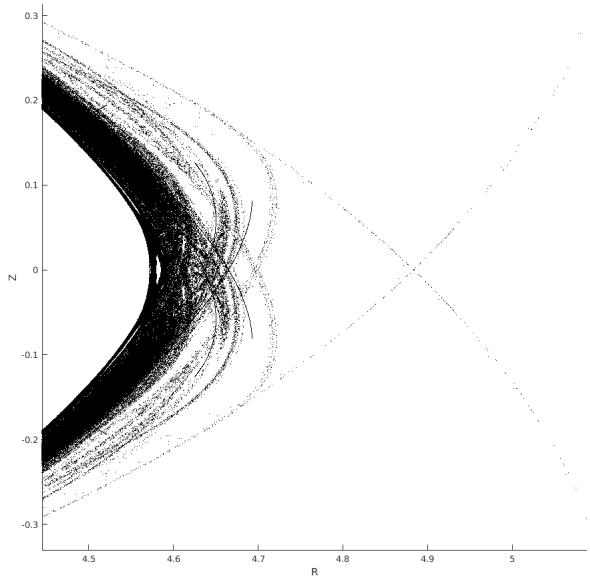

(2) *Right X point*

Figure 8: *X points in* $\varphi = 18°$ *plane*

Next we want to study the Rotational Transform of the fieldlines in the central region. To do so we need to find the magnetic axis, the fieldline that closes after one toroidal turn and around which all closed flux surfaces in the vicinity are concentric. This was also done by trial and error. The main finding here is that this axis is not circular, it has a toroidal helix structure much like the the coils producing the magnetic field, but this time with $N = N_{FP} = 10$. This configuration, therefore, shows torsion. To see this I show a plot of the values of $R(\varphi)$ and $Z(\varphi)$ for the magnetic axis:

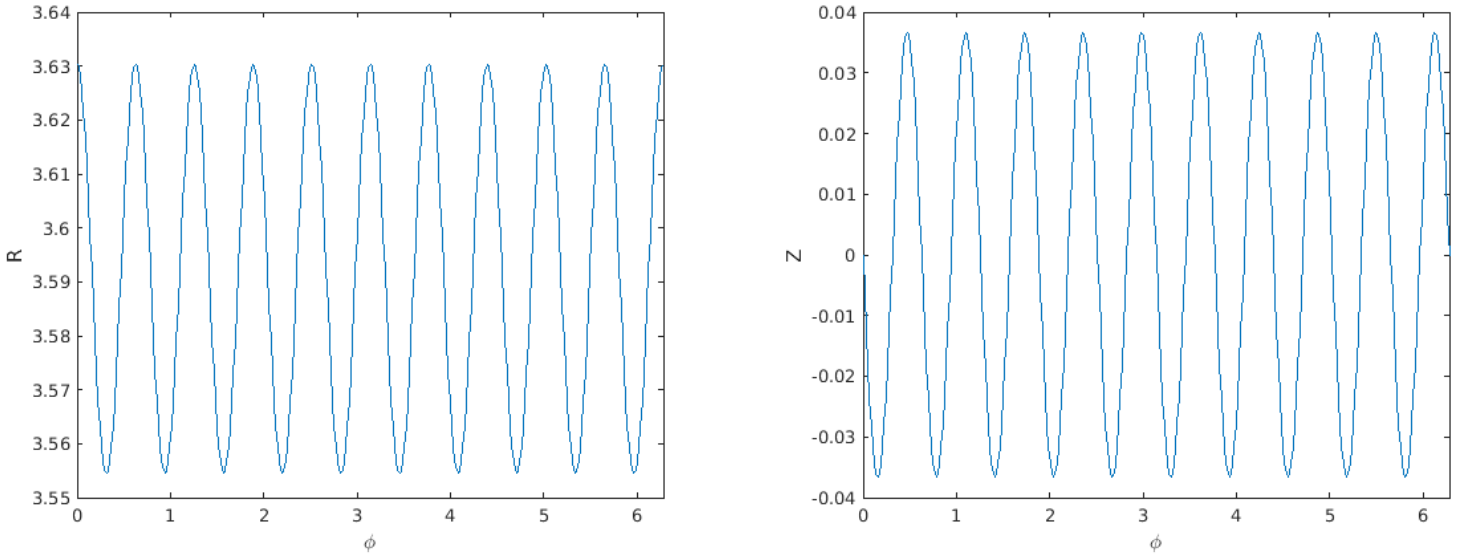

(1) $R(\varphi)$ **(2)** $Z(\varphi)$

Figure 9: *R and Z as functions of φ in one toroidal turn for the magnetic axis*

Upon analysis of these we have confirmation that this fieldline is indeed the magnetic axis, as it has the same value at $\varphi = 0, 2\pi$. The counter clockwise helical structure with $N = 10$ can be seen by noting that the two functions oscillate in such a way that the phase of R is $\frac{3\pi}{2}$ ahead of that of Z and have 10 periods per toroidal turn.
The magnetic axis oscillates around $R = 3.5922$ and $Z = 0$. This will be important when we re-scale the configuration.
Finally, we have now a fieldline with respect to which we can faithfully calculate the rotational transform, shown here as a function of the effective radius - the root mean squared distance to the magnetic axis of points in a flux surface. This effective radius acts as a flux surface label,

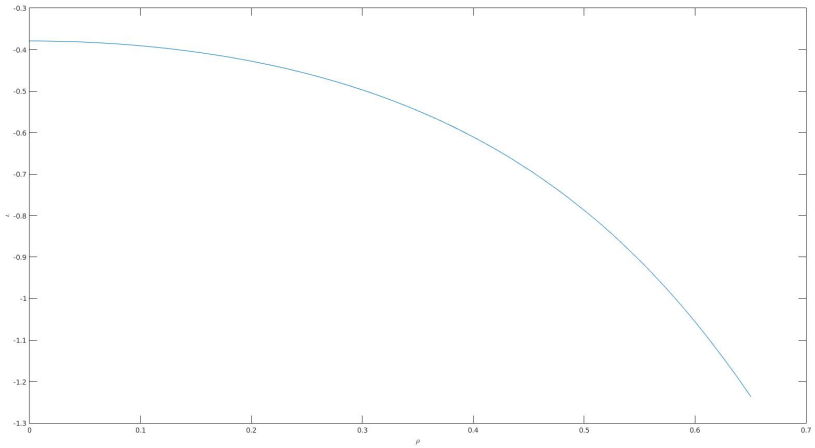

Figure 10: *Rotational Transform as a Function of the effective radius*

The Rotational Transform is, as expected, monotonous in the effective radius, and grows in absolute value. The negative sign simply indicates that fieldlines wind counterclockwise around the magnetic axis. It is worth mentioning that, to calculate this rotational transform I used 1000 fieldlines in the central region, with initial radius starting in the magnetic axis and ending at an approximate initial condition for the last closed flux surface (the boundary between regions). Here is a Poincaré plot of these fieldlines in the vicinity of the magnetic axis for $\varphi = 0$

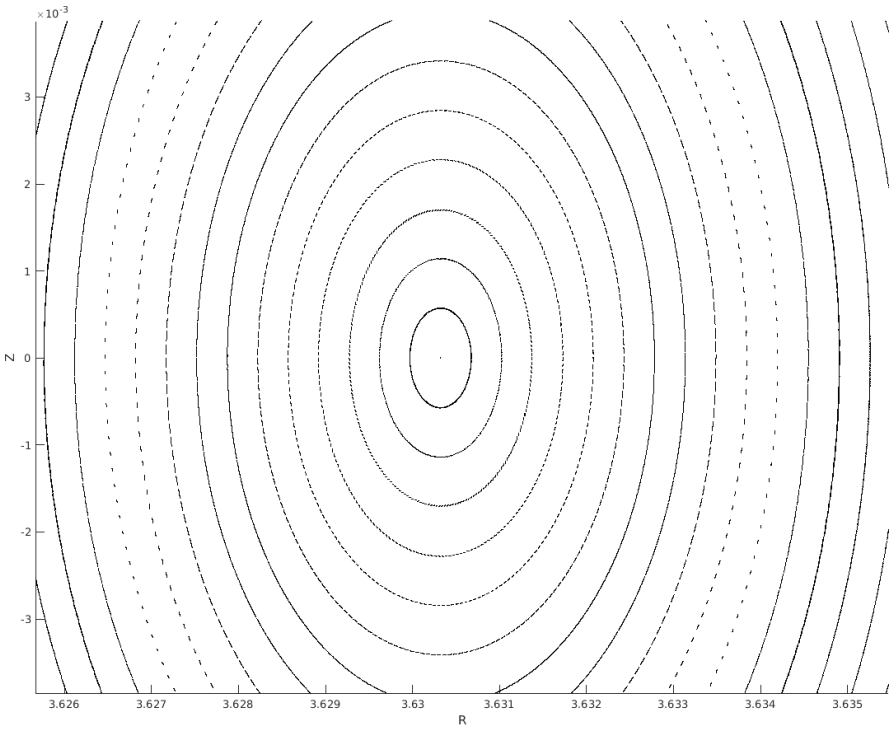

Figure 11: *Closed curves in the vicinity of the magnetic axis crossing the $\varphi = 0$ cutplane.*

It is known from Stellerator theory that the Rotational Transform in a torsionless stellerator for flux surfaces very close to the magnetic axis approaches a definite value depending on the ellipticity of the closed curves they form in a Poincaré Plot. The result is:

$$\iota(r_{eff} \to 0) = \frac{N_{FP}}{2} \frac{(r_{max} - r_{min})^2}{r_{min}^2 + r_{max}^2} \tag{11}$$

Where r_{min} and r_{max} are the ellipses major and minor radii. Upon inspection of the previous Poincaré Plot, one can obtain for the innermost ellipse $r_{min} \approx 4 \times 10^{-4}$ and $r_{max} \approx 6 \times 10^{-4}$. Which yields $\iota(r_{eff} \to 0) \approx \frac{20}{52} = 0.385$. This is in excellent agreement with the numerical estimate of $\iota \to 0.38$, in spite of the (now proven small) torsion exhibited by this configuration.

To end this section I show a plot of the magnetic axis viewed from the top and a plot of the last closed flux surface in 3D. The loops of current that generate this field can also be seen and have the same color code as before.

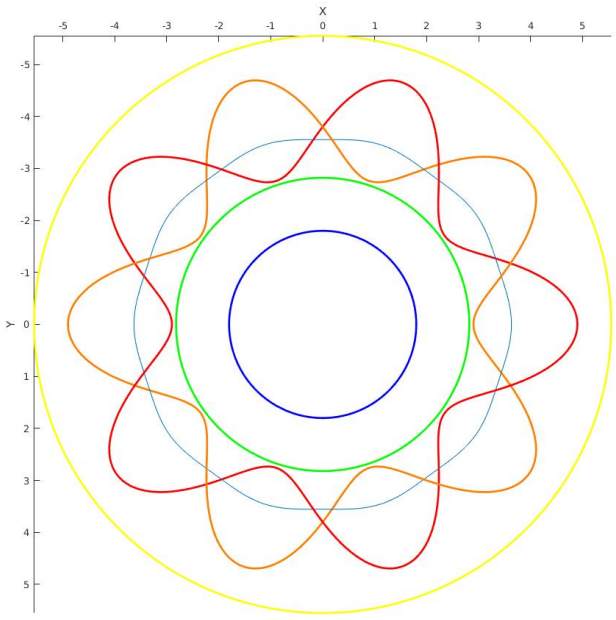

(1) *Magnetic Axis (light blue) top view*

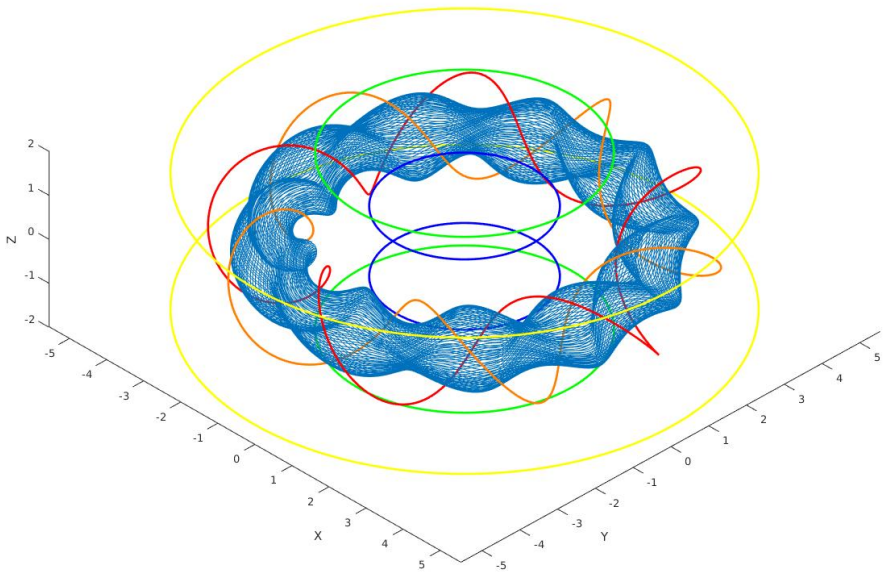

(2) *Last closed flux surface (light blue)*

3. Reduction of the system

As we have seen before, equations (6) are invariant under length scaling, meaning the that the geometry of the fieldlines is unchanged if we scale the whole system by a length factor, say R_0. Based on this, and inspired on the Poincaré Plots shown in article [6] (page 3), I decided to scale down the current loops by a factor R_0, in such a ways that the average value of R for the magnetic axis be unity. Therefore, every length in the system was scaled down by:

$$R_0 = 3.5922$$

I then rewrote the "coils." file and ran it through MAKEGRID, obtaining a magnetic field configuration. With FIELDLINES I followed this field and produced the same Poincaré plots as before, namely, for $\varphi = 0$:

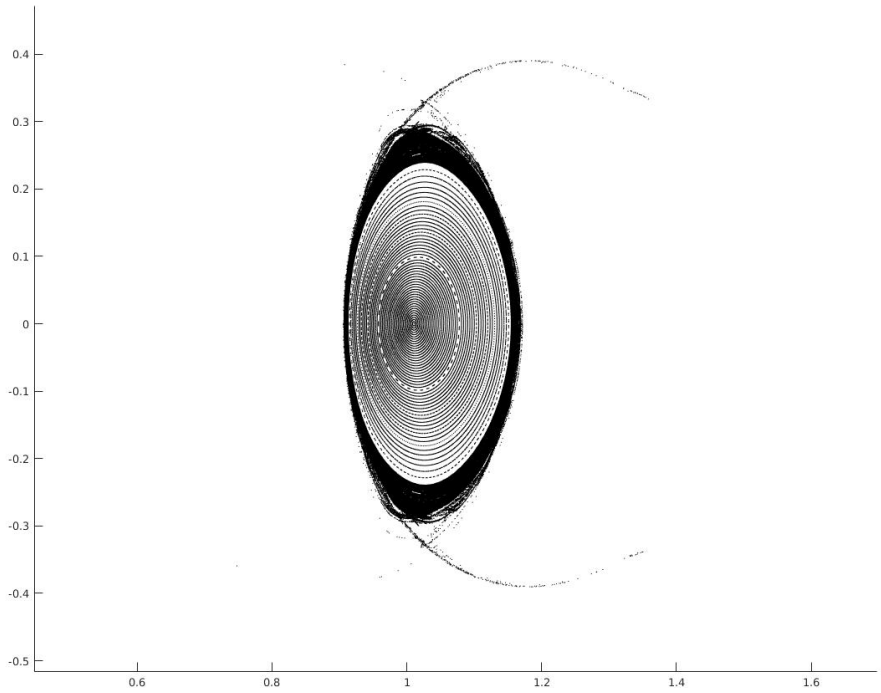

Figure 13: *Poincaré Plot for the reduced Magnetic Field configuration in the $\varphi = 0$ cutplane.*

Just as expected, this is exactly the same figure as before but now centered at $R/R_0 = 1, Z/R_0 = 0$.
But what is the point of reducing the system? Weren't we just fine with the original configuration? Well, reducing the volume of the simulation makes it more efficient computationally, that I can say. The simulations were much faster in the reduced system. However, the reason for this lies beyond the work I present in this report, and requires the answer to the question: why study the magnetic geometry of a stellerator in vacuum? Short answer: so that when we add plasma to the stellerator we have an approximate idea of where it will go, and how it will get there. On the boundary of a stellerator the plasma exhibits very complex turbulent behaviour. This plasma turbulence is an active research topic in Computational Plasma Physics. The knowledge we gain about this magnetic field geometry will help us in simulating said turbulent behaviour in the future, and for these simulations it is crucial that the volume be kept of order 1.

V. The Wall

In the last section I talked briefly about simulating turbulence in the boundary of a stellerator, but so far our stellerator is nothing but a set of currents and the magnetic field they generate. We need to give it a wall. For this my advisors gave me the following geometrical constraints:

1. The Cross Section of the wall must be Rectangular its area must be constant and minimal - why?, because our turbulence simulation codes work much better in a Cartesian grid, where boundary conditions are easily provided, with the minimum simulation volume.

2. The Wall must never touch any current loop - Obviously you don't want the current generating the magnetic field to go inside the vessel where all the hot plasma is located.

3. The wall can rotate poloidally about a circle of fixed R and Z.

The rest of my work, and also the main part of it, can be summarized by the next sentence:

Find a wall for the stellerator that obeys the constraints, in such a way that the fieldlines through which heat carrying charged particles leave the vessel strike it, mainly, in opposite sides (top and bottom) of each rectangular cross section.

I'll start by saying that, at the time of writing, I have not found such a wall for the stellerator, but I will discuss the ideas I have pursued so far.

1. Toroidal Helix Rotating Rectangle Wall

The motivation for this is simple: It is a wall of rectangular cross section that rotates with the flux surfaces. Each point in the wall traces out a toroidal helix. Since the magnetic axis rotates around $R = 1, Z = 0$ I chose this circle as the axis of poloidal rotation for the wall. And finally, because the flux surfaces rotate counter clockwise with a toroidal period of $\frac{2\pi}{5}$ (remember that the whole structure morphs back into its original self after rotating poloidally 180° in one toroidal field period of $\frac{2\pi}{10}$), the wall must accompany this change:

Mathematically, a rectangular contour centered in $R = 1, Z = 0$ of width a and height b laying parallel to the z axis is defined as the set of points such that:

$$\mathcal{R}_0 = \{(R, Z) \in \mathbb{R}^2 : (R - 1 = \pm a/2 \wedge -b/2 \leq Z \leq b/2) \vee (Z = \pm b/2 \wedge -a/2 \leq R - 1 \leq a/2)\} \tag{12}$$

If you assume this to be the cross section boundary at the $\varphi = 0$ plane then the cross section boundary at some other cutplane φ is:

$$\mathcal{R}_\varphi = \left\{(R, Z) \in \mathbb{R}^2 : \begin{pmatrix} R-1 \\ Z \end{pmatrix} = \begin{pmatrix} \cos(-5\varphi) & -\sin(-5\varphi) \\ \sin(-5\varphi) & \cos(-5\varphi) \end{pmatrix} \begin{pmatrix} R^*-1 \\ Z^* \end{pmatrix} \quad , \quad (R^*, Z^*) \in \mathcal{R}_0 \right\} \tag{13}$$

Graphically:

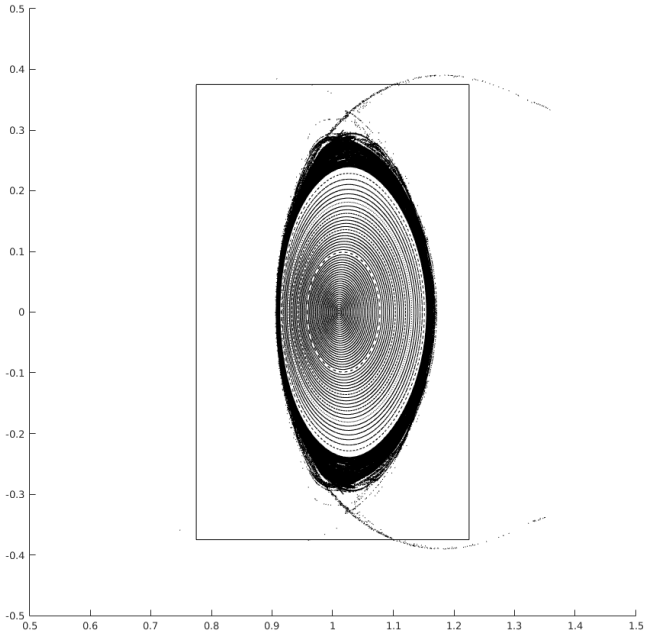

(1) *Cutplane* $\phi = 0°$

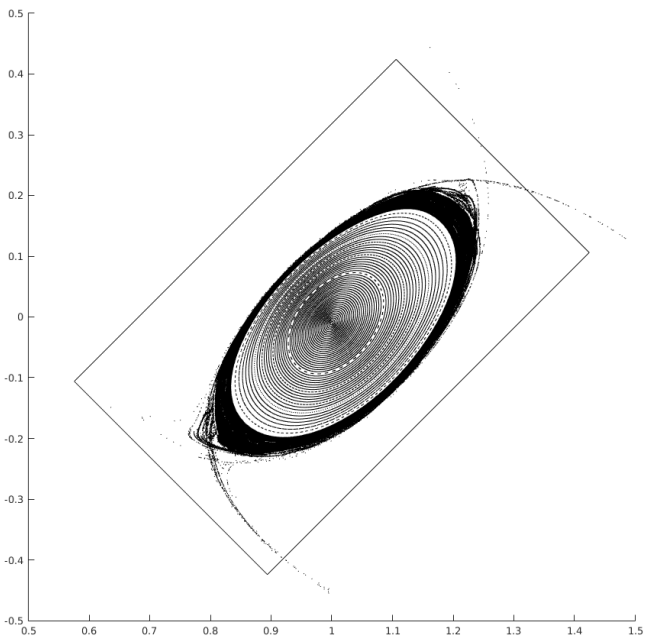

(2) *Cutplane* $\phi = 9°$ *- counter clockwise rotation of* $45°$

Figure 14: *Wall and Poincaré Plot*

The Rectangle cross section in the previous plots has $a = 0.45$ and $b = 0.75$. As we can see from the right plot, the legs of the double null don't intersect the rectangle in opposing sides everywhere, and since these legs are the fieldlines through which the plasma exits the vessel, in principle fails our request in principle. However, I did not reach this conclusion during the project time and went on with studying where various fieldlines strike this particular wall and how long they stay inside it.

1.1 Fieldlines going through $\varphi = 0$

I followed fieldlines that start in the $\varphi = 0$ cutplane (inside the vessel cross section) forwards and backwards, and asked STELLOPT to keep track of the striking points only (-hitonly option when running FIELDLINES), for efficiency. The connection length plot for these initial conditions is:

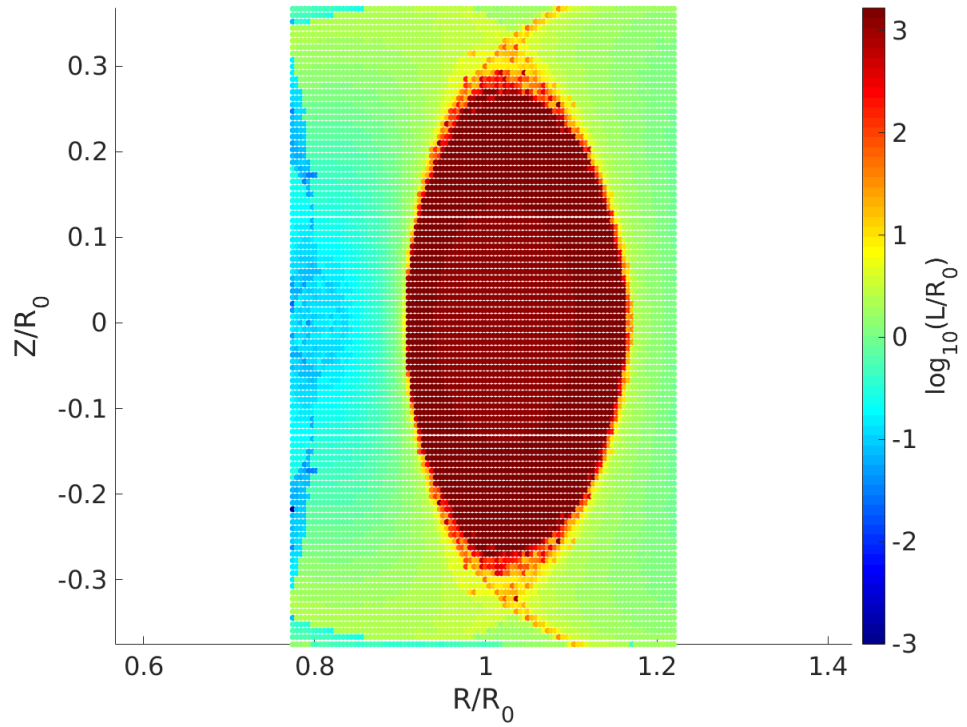

Figure 15: *Connection length L for Fieldlines going through* $\varphi = 0$

This plot is a nice illustration of what I discussed in section II.1.2. There are three types of fieldlines. Those starting in a Red point never leave the stellerator ($log_{10} \approx 3$ because I followed each fieldline 100 times around the torus forward and backward implying $L \sim 100 * 2 * 2\pi \sim 10^3$). Those starting in a yellowish orange point leave the vessel after some turns. Finally those in Green/Blue Points leave immediately (eventually going to infinity or closing outside the vessel). We are very interested in those starting in Orange/Yellow points, as it is them who carry the heat away.

Next I looked for the striking points of fieldlines that leave the vessel, discarding, based on the final angle, those that don't. Noticing that a point in the wall can be labeled by 2 coordinates, the toroidal and poloidal angles φ and $\theta = \arctan(Z/(R-1))$ we can represent strikepoints as points in the (φ, θ) plane. However, we need a way to differentiate between a points (more concretely a triangular patch according to our wall discretization technique) striked by a different number of fieldlines. This is well done through colorcoding, like in the case of the connection length.

In addition to this, there is a very important property of the Stellerator field we can exploit to gain more insight. Since the field configuration is the same in every period, if one fieldline going through (R_1, φ_1, Z_1) hits the wall at $(R_1^W, \varphi_1^W, Z_1^W)$, then a fieldline going through $(R_1, \varphi_1 + \frac{2\pi}{10}, Z_1)$ will hit the wall at $(R_1^W, \varphi_1^W + \frac{2\pi}{10}, Z_1^W)$. This property ensures that, to find the strike points everywhere it is only necessary to study fieldlines starting in one period. Once their strikepoints are known we can assume that for each of them, there are $N_{FP} - 1 = 9$ other strikepoints separated in φ by a multiple of $\frac{2\pi}{10}$. Therefore one point in the (φ, θ) plane has 9 other brothers at $(\varphi + k\frac{2\pi}{10}, \theta)$, $k = 1, ..., 9$. Here is the difference between the (φ, θ) strikepoint map with and without this nontrivial addition:

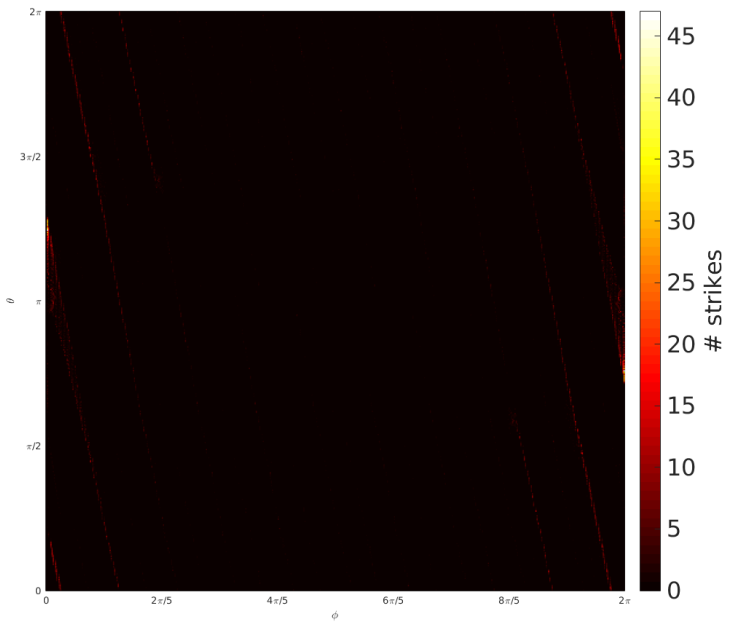

(1) *Strikepoint map with only one period*

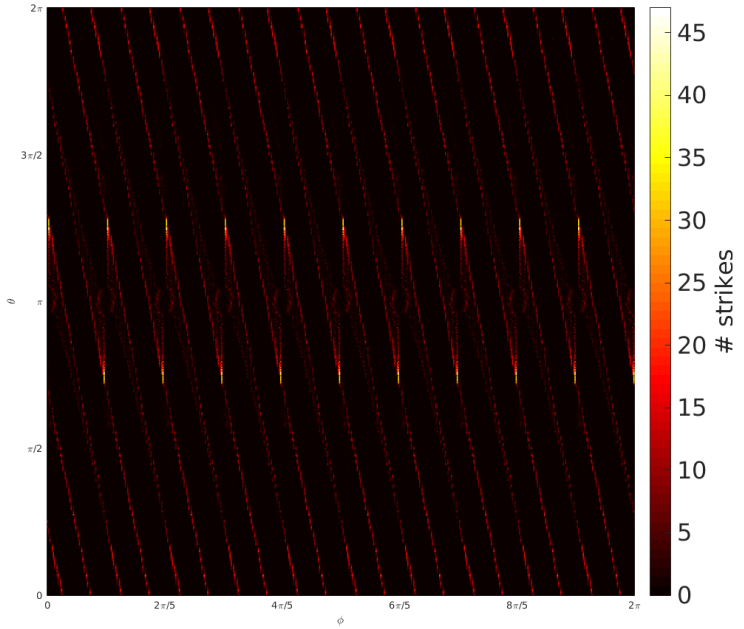

(2) *Strikepoint map with all 10 periods*

On the left figure the strike points are very faint dots that are barely visible (especially when displayed here because of image compression). When considering strikepoints of fieldlines starting in all $\varphi = k\frac{2pi}{10}$, $k = 1, ..., 10$ cutplanes, a pattern of lines of slope ≈ -5 appears. This tells us that we are in the good path, since this is exactly the kind of pattern expected for a wall co-rotating with the magnetic field. It is still very hard to tell if in which sides of the rectangular cross section do these fieldlines strike the wall. To elucidate this, all we have to do is "untwist" the wall, or by other words, measure the poloidal angle with respect to a line that is fixed in the frame rotating with the rectangular cross section. This just amounts to sending:

$$\theta \to \theta - (-5\varphi) \quad , \quad \text{modulo } 2\pi \tag{14}$$

Performing this trick, the strikepoint map is:

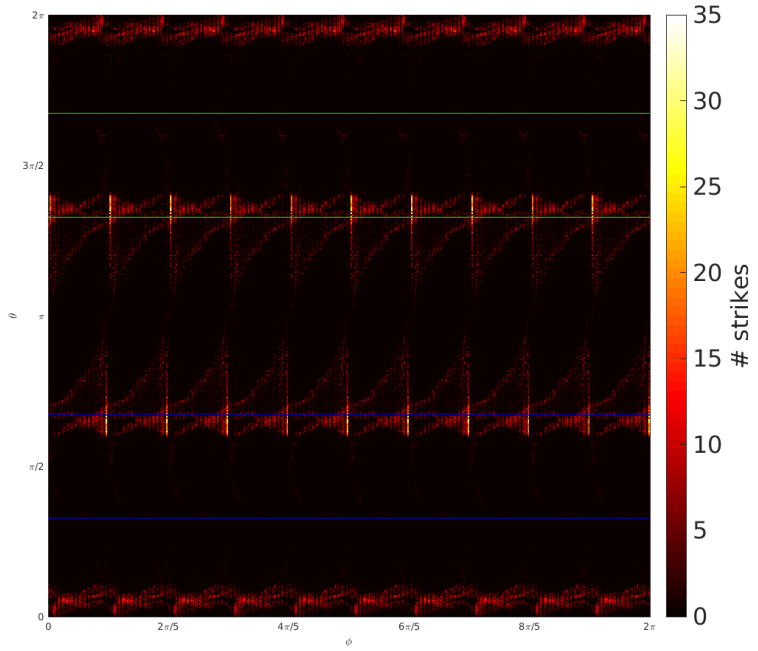

Figure 17: *Strikepoint map after untwisting the wall and adding all 10 periods*

I have added, for convenience, 2 blue lines delimiting the top of the rectangle and 2 green lines delimiting the bottom. As you can see these fieldlines hit the wall about everywhere, but the side of the rectangle that is striked the most (by the fieldlines I followed of course, since there is an equal and infinite number of fieldlines striking the wall in any given patch) is the left one (see figure 14). This is expected since, from the connection length plot this is the side closest to which a lot of fieldlines with short connection length start (green/blue points).

1.2 Fieldlines going through $Z = 0$ plane

I also looked at the fieldlines that go through the $Z = 0$plane and how they hit the wall. The procedure was exactly the same. I obtained the following connection length Plot:

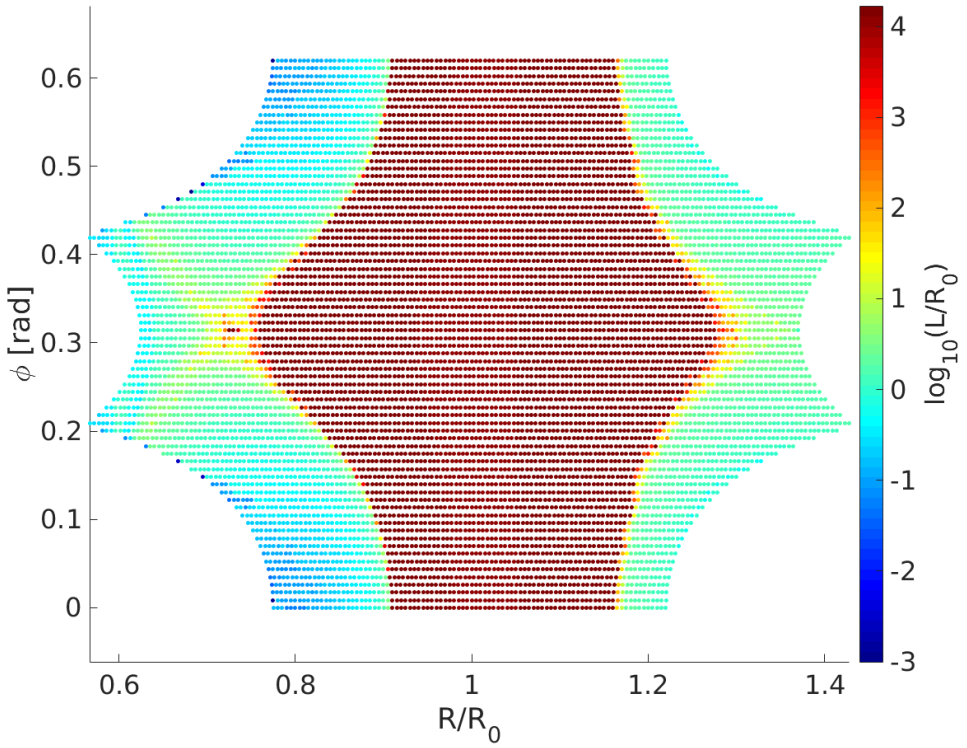

Figure 18: *Connection length L for Fieldlines going through $Z = 0$ plane*

The plot has this shape because I only followed fieldlines that start inside the vessel. Notice also that the maximum connection length is 10^4 because in this case I followed fieldlines 1000 turns around the torus instead of 100. The strike point map, after repeating periods and untwisting the wall, is:

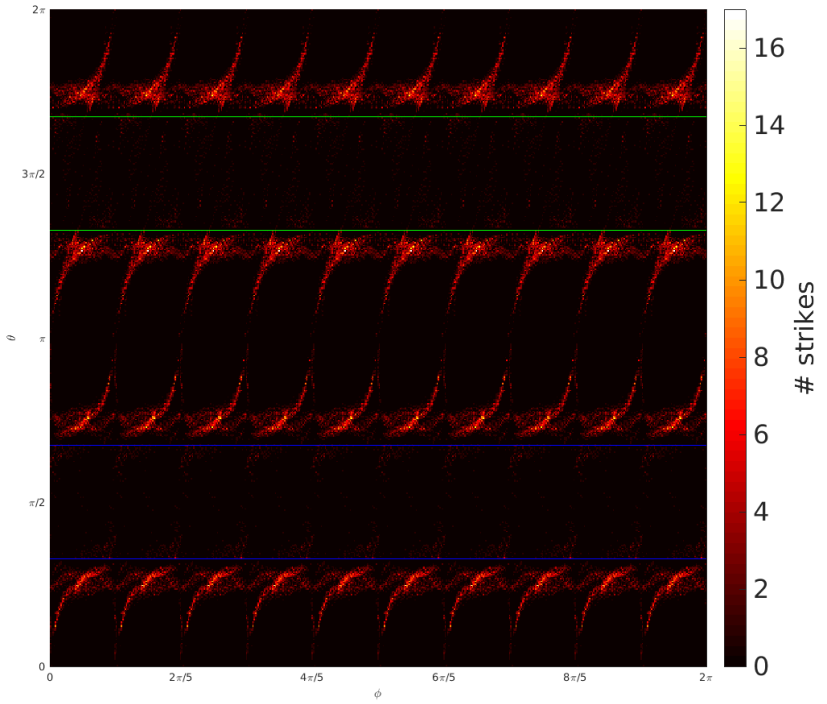

Figure 19: *Strikepoint map after untwisting the wall and adding all 10 periods*

We have again that most fieldlines strike the left and right sides of the rectangle in figure 14. Although a few fall between the green lines and between the blue lines (bottom and top).

After all this research I realized I was in the wrong path to finding a good wall because I was looking at the strike points of the wrong fieldlines, not representative of heat. A hot fieldline is one that carries energetic charged particles out of the vessel. Instead of looking at every fieldline's strike point I should first find which of them are hot and which of them are cold (not hot), and then follow the hot ones. The work done so far has not been useless though, because the connection length plot can tell us where do the hot fieldlines - at orange/yellow points.

1.3 Fieldlines starting in the separatrix region

So far, we have concluded that we need only to track the strikepoints of hot fieldlines. The connection length plot in figure 15 tells us where they cross the $\varphi = 0$ axis (orange/yellow points). We are, therefore, in need of a way to tell STELLOPT to follow fieldlines that start at these points. Noticing that this region - the separatrix region - has a sort of elliptical shape, I decided to find a set of ellipses that covered most of it and then sample initial conditions for my fieldlines from this set. Here is the connection length plot for the fieldlines starting in this set:

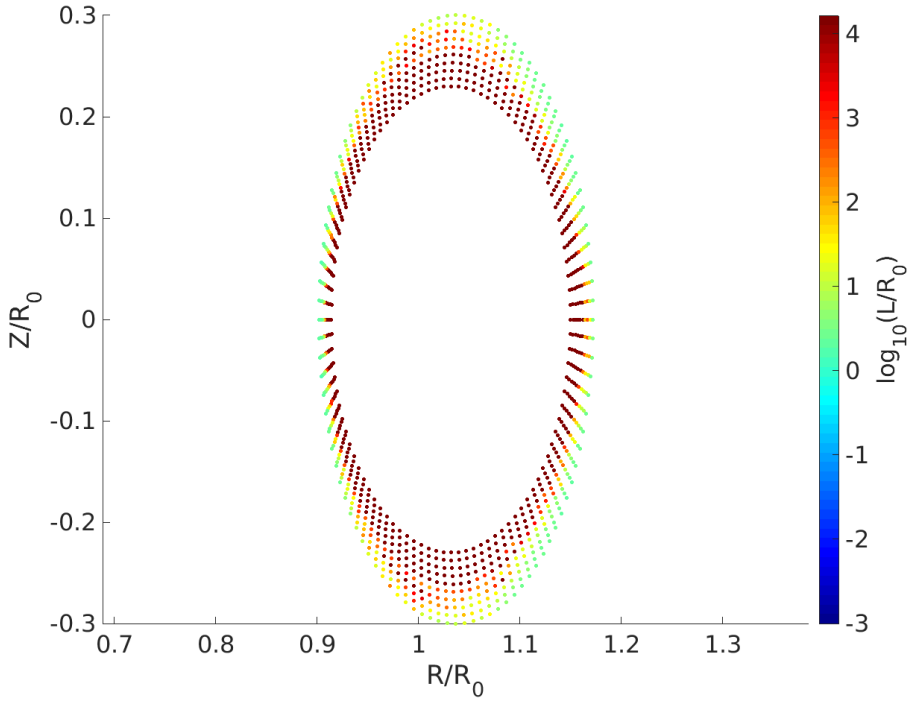

Figure 20: *Connection length L for fieldlines going through the separatrix region in $\varphi = 0$ plane*

And the strikepoint map:

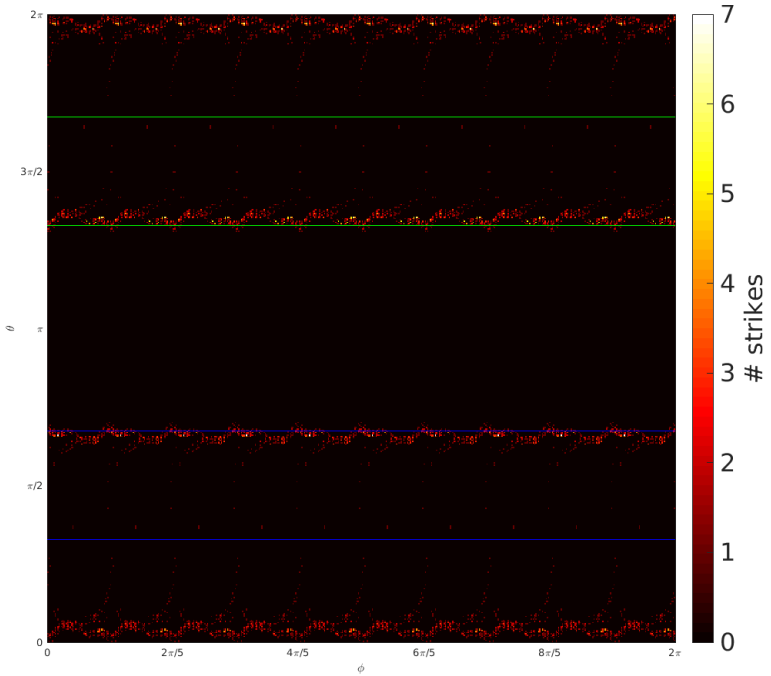

Figure 21: *Strike Points for fieldlines going through the separatrix region in $\varphi = 0$ plane*

So far we have a big improvement, no fieldlines strike the left side of the rectangle and most strike points are located in the top and bottom sides (opposite sides). There is however, still a relatively high density of strike points around $\theta = 0$, which I presume correspond to the fieldlines I follow that begin in green points, but we still have no way of knowing which fieldlines correspond to which strikepoints. In spite of this, we see that a lot of fieldlines strike right in the corners of the rectangular cross sections. This is a primary thing to avoid, as it will make turbulence simulations in the boundary of this wall more likely to crash. As a result, I decided to change the rectangular cross section's height and width to a = 0.4 and b = 0.64. These numbers were chosen by looking at the Poincaré Plots of fieldlines starting in the separatrix (in the absence of the wall) and trying to fit the whole magnetic structure inside a rectangle in such a way that only the legs intersect the rectangle's sides, doing so on the top and bottom. This has to be true in all cross sections, namely when $\varphi = 18°$, where satisfying this poses more problems.

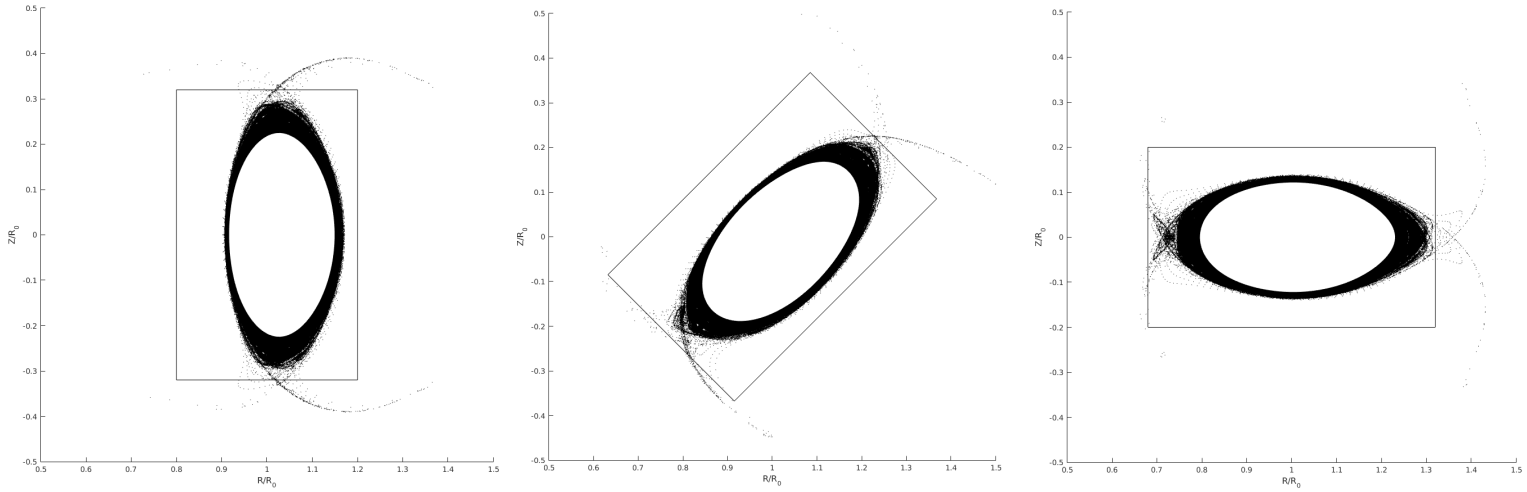

(1) $\varphi = 0°$ *cutplane*

(2) $\varphi = 9°$ *cutplane*

(3) $\varphi = 18°$ *cutplane*

These rectangles seem to be an improvement, so I repeated the process, follow fieldlines, get the connection length and strikepoint map. This time, though, I followed 10 times more fieldlines.

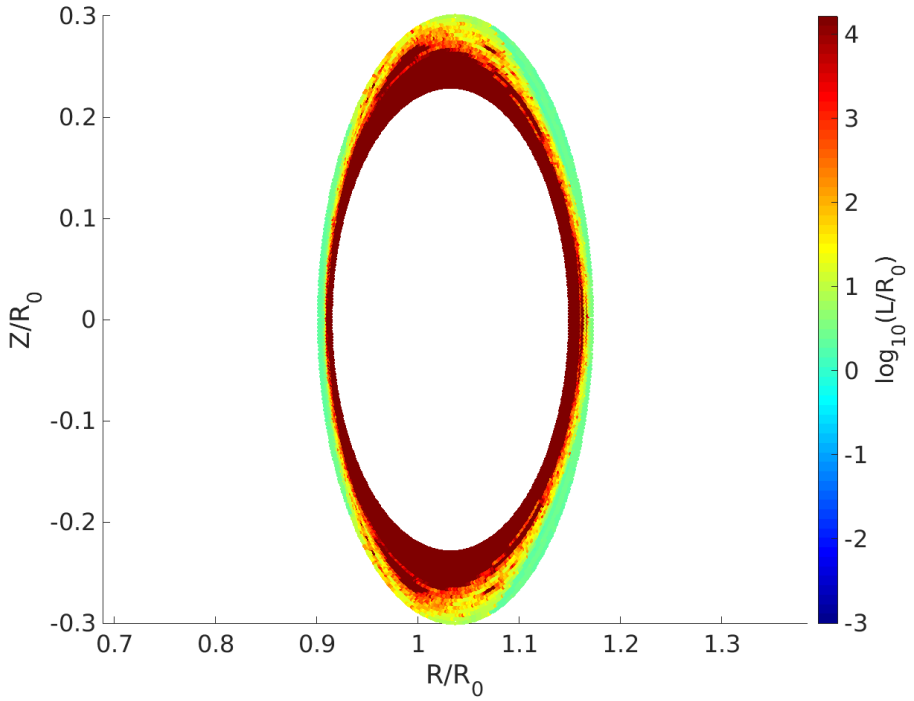

Figure 23: *Connection length L for fieldlines going through the separatrix region in $\varphi = 0$ plane*

For the strike point map lets try to be a bit more smart and plot only strikepoints of fieldlines that start at yellow / orange points by **explicitly** asking MATLAB to filter out, based on their connection length, those who don't. This is what I should have been doing all along but only though of it at the end! Looking at the connection length plot in figure 23 we see that $log_{10}(L) \gtrapprox 1.3$ for yellow/orange so let's just plot the striking points of fieldlines in that connection length range, as those are the ones that carry the heat out of the vessel.

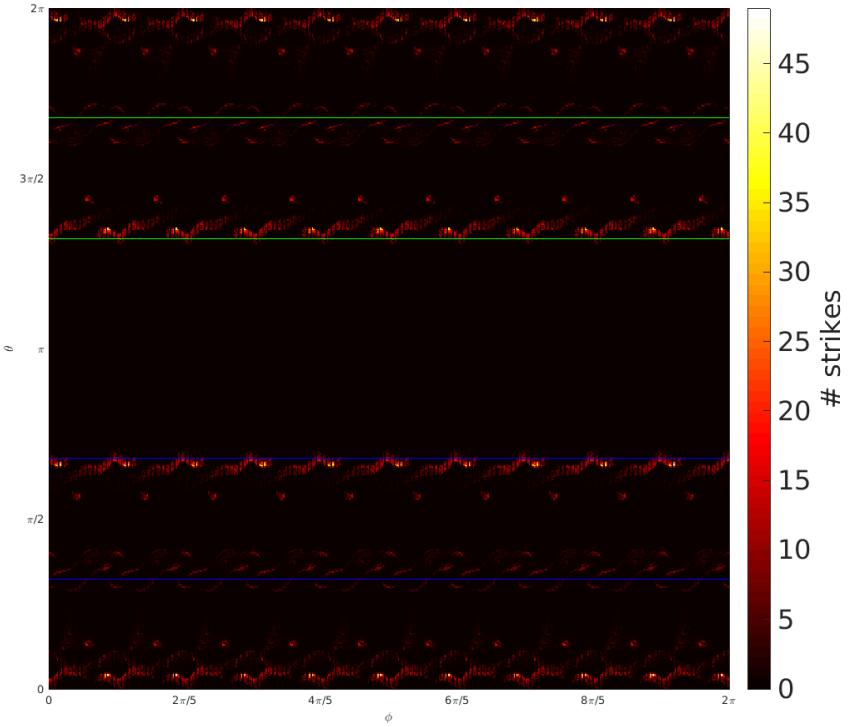

Figure 24: *Strike Points for fieldlines going through the separatrix region in $\varphi = 0$ plane with restricted to $log_{10}(L) \gtrapprox 1.3$*

Notice that, contrary to what I presumed, there are still quite a lot of strikepoints close to $\theta = 0$. And since we are now sure that they come from fieldlines that have $log_{10}(L) \gtrapprox 1.3$, these are striking points of hot fieldlines. Just as a check, lets go back to the connection length plots for fieldlines starting in $\varphi = 0$ and $Z = 0$: figures 15 and 18, and see that the heat carrying fieldlines also have $log_{10}(L) \gtrapprox 1.3$. Asking MATLAB to only plot their strike points, we expect the strikepoint map to be very different from figures 17 and 19, respectively. Indeed we find:

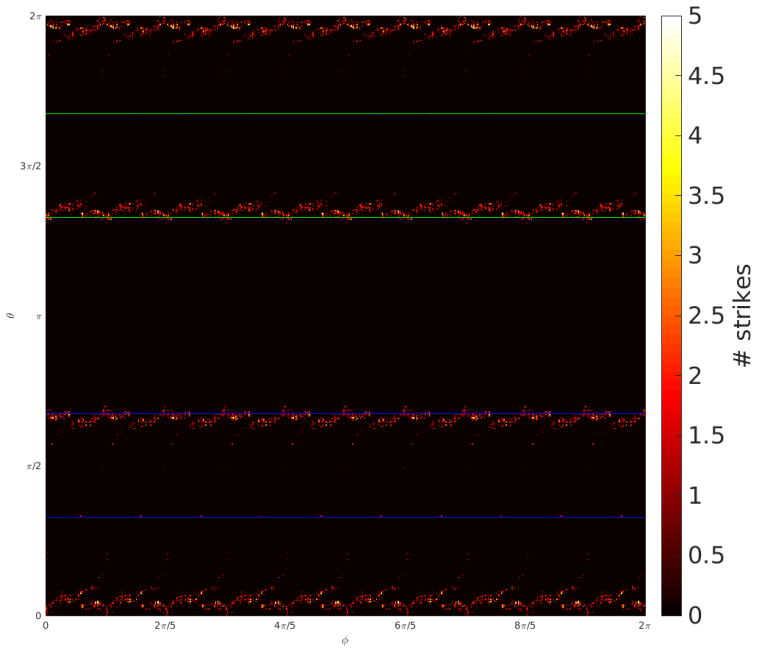

(1) *Strikepoint map for the hot fieldlines in figure 15*

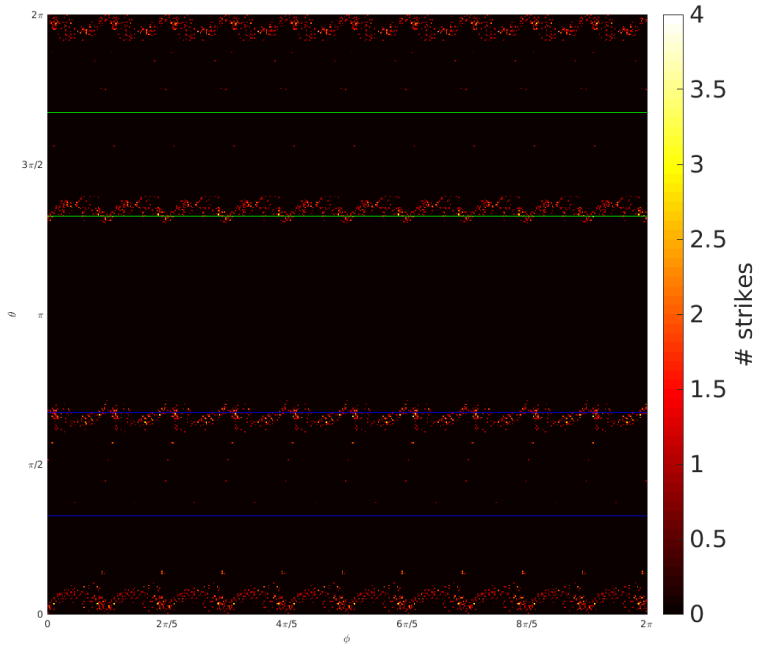

(2) *Strikepoint map for the hot fieldlines in figure 18*

This is very different from what we were looking at previously. Indeed, we managed to find where the hotter fieldlines strike and obtained a similar map to the one in figure 24. There are no fieldlines hitting the left side of the rectangles, meaning the majority of strikepoints in figures 17 and 19 come indeed from cold fieldlines. Notice, however, the reduced number of strikes in the last 2 figures compared to what we obtained in 24. Looking only at the separatrix region really helps to outline statistically where fieldlines hit the most. In spite of this, the new wall improves a bit but didn't get rid of the main problem - hot fieldlines are still striking the corners of the rectangle.

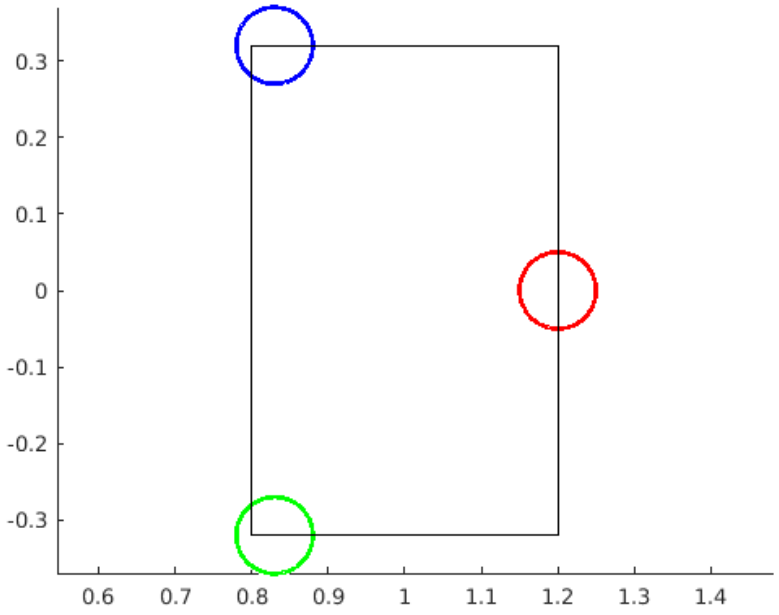

Figure 26: *Main points of hot fieldline strike density in the rectangular contour of the wall*

2. Overview of the last section

To summarize all the things I tried in the last section I present the following procedure to decide if a given toroidal Helix Wall is suitable or not. By suitable I mean that hot fieldlines don't strike its corners, and ideally only hit the top and bottom of the wall. Given magnetic fieldlines starting in the $\varphi = 0$ plane with $Z = 0$:

1. Find a rectangular cross section (width a and height b), a center point and a rotation period such that the resulting wall "contains" the Poincaré Plot in every cutplane like in figure 14. Only the legs can stick out of the rectangle.
2. Find initial conditions for the separatrix fieldlines by making a connection length plot like 15. This set of points is called the separatrix region.
3. Think of a way to sample as many points in the separatrix region as possible, to obtain good statistics. These will be the initial conditions for the hot fieldlines. In my case I used ellipses but this is not necessary.
4. Make a connection length plot for those fieldlines and decide a connection length limit. Fieldlines whose connection length is below this are cold. Above this they are hot. In my case I went for $log_{10}(L_{min}) = 1.3$
5. Plot the strikepoint map for the hot fieldlines.
6. Make use of stellerator field symmetry and repeat the strike points by shifting in φ. Move to the frame rotating with the rectangle - untwist the wall and plot the strikepoints.
7. Identify the corners of the cross section and decide if the wall is suitable or not, based on the density of fieldlines that strike them
8. Identify the corners of the cross section and decide if the wall is suitable or not, based on the density of fieldlines that strike them.

.

VI. Final thoughts and conclusions

During this semester project I learned a lot about how to numerically look into stellerator magnetic field models and which configurations have certain desired properties and which don't. Studying a model for the LHD's rotating double null structure, by making Poincaré plots, really proved useful to describe where this field is expected to confine the plasma and where it doesn't. I then focused my work on trying to see where this field is expected to direct hot plasma particles and managed to come up with a shape for a wall that satisfies all the geometrical constraints given to me by my advisors. I then looked at where in the wall the magnetic field is expected to divert plasma particles and found that this happens near the corners of each cross section. This is unwanted, and I have yet to find a wall that, while satisfying all the constraints is not striked by fieldlines at its corners. Although I found a way to, given a wall, see if hot fieldlines hit its corners or not, I would like to briefly discuss a better method for doing so. I did not pursue this method in this semester but am hoping to continue my search for a suitable wall for a particular configuration using it:
In the final section I came to the realization that the connection length is a good indicator of how hot a particular field line is. The new method will consist in following fieldlines that start as close as possible to the wall boundary in both directions and look at their connection length. I expect most of them have a relatively small connection length, but those that don't must go inside the torus in one direction for a relatively long distance, and must, therefore, be hot. Initial conditions for hot fieldlines will be identified as their strike points. By virtue of stellerator and wall symmetry, it will only be needed to follow fieldlines that start in a range of $\Delta\varphi = \frac{2\pi}{10}$.

References

[1] https://princetonuniversity.github.io/STELLOPT/STELLOPT. html

[2] https://princetonuniversity.github.io/STELLOPT/

[3] https://princetonuniversity.github.io/STELLOPT/MAKEGRID

[4] https://princetonuniversity.github.io/STELLOPT/FIELDLINES

[5] Freiberg: Plasma Physics and Fusion Energy

[6] Yasushiro Suzuki. Effect of pressure profile on stochasticity of magnetic field in a conventional Stellerator.

[7] H. Yamaguchi. A quasi-isodynamic magnetic field generated by helical coils